



UWL REPOSITORY
repository.uwl.ac.uk

Coupling Behaviour of Autogenous And Autonomous Self-Healing Techniques
for Durable Concrete

Shaaban, Ibrahim ORCID logo ORCID: <https://orcid.org/0000-0003-4051-341X> (2024) Coupling Behaviour of Autogenous And Autonomous Self-Healing Techniques for Durable Concrete. International Journal of Civil Engineering, 22. pp. 925-948. ISSN 1735-0522

<http://dx.doi.org/10.1007/s40999-023-00931-4>

This is the Accepted Version of the final output.

UWL repository link: <https://repository.uwl.ac.uk/id/eprint/10629/>

Alternative formats: If you require this document in an alternative format, please contact: open.research@uwl.ac.uk

Copyright: Creative Commons: Attribution 4.0

Copyright and moral rights for the publications made accessible in the public portal are retained by the authors and/or other copyright owners and it is a condition of accessing publications that users recognise and abide by the legal requirements associated with these rights.

Take down policy: If you believe that this document breaches copyright, please contact us at open.research@uwl.ac.uk providing details, and we will remove access to the work immediately and investigate your claim.

Rights Retention Statement:

Coupling Behaviour of Autogenous And Autonomous Self-Healing Techniques for Durable Concrete

Ahmed Hassanin^{1,2}, Amr El-Nemr³, Hesham F. Shaaban⁴, Messaoud Saidani⁵
and Ibrahim Shaaban^{6,*}

aihnnng@missouri.edu¹, ahmed-ibrahim@eru.edu.eg², amr.elnemr@guc.edu.eg³,
hmshaban@eng.zu.edu.eg⁴, cbx086@coventry.ac.uk⁵, ibrahim.shaaban@uwl.ac.uk⁶

Abstract

Recent research on self-healing concrete has shown some drawbacks and conflicts between the different techniques such as difficulty in casting, healing agent release, preparation complexity, high safety requirements against bacteria protection, undesirable expansion, and uncertainty in healing product generation. Despite these limitations, the hybrid technique was suggested and showed promising results. This paper explores the hybridization of the two techniques; autonomous and autogenous by utilizing the *B. subtilis* bacteria, mineral admixtures like fly ash, and Polyvinyl alcohol fibers (PVA) together. The experimental program involves assessing the self-healing efficiency when coupling the bacteria, fly ash, and PVA fiber by assigning six mixtures, including a control OPC. The six mixtures encountered the Bacteria addition at certain concentrations and varying PVA fiber percentages; 1, 1.5, and 2% while partially replacing the cement replacement with 20% fly ash, while the last mixture combines both the bacteria, fly ash and 1% PVA fiber. Mechanical properties such as compressive and flexural strength, in addition to, water absorption and sorptivity as transport properties were examined for concrete repair and restoration purposes. The results reveal that the *B. subtilis* bacteria significantly enhance the compressive and flexural strength recovery along with lowering sorptivity and absorption rate compared to those with PVA addition when exposed to wet and dry cycles of curing at 28 days of age. The coupling effect, on the other hand, provides a substantial gain in strength of 63% at a longer age (56 days), indicating the potential of this approach for long-term concrete repair. Despite the challenges of the *B. subtilis* survival bacteria, the coupling of both bacteria and PVA fiber demonstrates superior performance in maintaining the durability of repaired concrete in the long term.

Keywords: self-healing techniques; absorption; durability; mechanical properties; concrete repair; crack widths.

Compliance with Ethical Standards

- The authors declare that they have no conflict of interest.
- This article does not contain any studies with human participants or animals performed by any of the authors.
- The authors declare that they have no known competing financial interests or personal relationships that could have appeared to influence the work reported in this paper.
- The authors state that they did not get any funding for this research and it is self-funded.

¹ Postdoctoral Fellow, Civil and Environmental Engineering Dept., University of Missouri-Columbia, USA.

² Lecturer, Engineering Construction Dept., Faculty of Engineering, Egyptian Russian University-Cairo, Egypt.

^{3,*} Associate Professor in Material Engineering, Civil Engineering Program, German University in Cairo (GUC), Cairo, Egypt.

⁵ Professor of Structural Engineering and Dean, National Zagazig University, Egypt.

⁵ Associate Director of Research and Engagement, Coventry University, UK.

^{6,*} Programme Director, University of West London, UK.

Coupling Behaviour of Autogenous And Autonomous Self-Healing Techniques For Durable Concrete

Abstract

Recent research on self-healing concrete has shown some drawbacks and conflicts between the different techniques such as difficulty in casting, healing agent release, preparation complexity, high safety requirements against bacteria protection, undesirable expansion, and uncertainty in healing product generation. Despite these limitations, the hybrid technique was suggested and showed promising results. This paper explores the hybridization of the two techniques; autonomous and autogenous by utilizing the *B. subtilis* bacteria, mineral admixtures like fly ash, and Polyvinyl alcohol fibers (PVA) together. The experimental program involves assessing the self-healing efficiency when coupling the bacteria, fly ash, and PVA fiber by assigning six mixtures, including a control OPC. The six mixtures encountered the Bacteria addition at certain concentrations and varying PVA fiber percentages; 1, 1.5, and 2% while partially replacing the cement replacement with 20% fly ash, while the last mixture combines both the bacteria, fly ash and 1% PVA fiber. Mechanical properties such as compressive and flexural strength, in addition to, water absorption and sorptivity as transport properties were examined for concrete repair and restoration purposes. The results reveal that the *B. subtilis* bacteria significantly enhance the compressive and flexural strength recovery along with lowering sorptivity and absorption rate compared to those with PVA addition when exposed to wet and dry cycles of curing at 28 days of age. The coupling effect, on the other hand, provides a substantial gain in strength of 63% at a longer age (56 days), indicating the potential of this approach for long-term concrete repair. Despite the challenges of the *B. subtilis* survival bacteria, the coupling of both bacteria and PVA fiber demonstrates superior performance in maintaining the durability of repaired concrete in the long term.

Keywords: self-healing techniques; absorption; durability; mechanical properties; concrete repair; crack widths.

1. Introduction

Concrete exhibits cracking as the sustained service load is applied which develops tensile stresses at the extreme fiber of the beam element or excessive compression load on compression element as columns. These cracks might inevitably find their path through the porousness of the concrete. Hence, this cracking would shorten the durability and damage the endurance life of the structures, in addition to the maintenance cost that would be required to repair or rehabilitate the damaged structure [1]. Eventually, this cracking has different causes and possesses various paths, however, they commonly start internally through microcracking and end up with concrete fracture, in addition to steel reinforcing bars experiencing corrosion, especially structures in coastal areas [2]. Generally, infrastructures that are more than 50 years old are susceptible to deterioration and comprehensively require maintenance [3]. Japan adopted self-healing as a promising technique when dealing with inherent cracks in concrete elements [4, 5].

43 The self-healing techniques are divided into two main techniques; autogenic and
44 autonomic self-healing of the concrete. Several investigations reported that small cracks in
45 concrete can heal under the effect of 'autogenous healing' or 'self-healing' of concrete.
46 Usually, this action takes place through, physical, and mechanical processes of the concrete
47 mix ingredients based on calcite crystallization to form calcium carbonate along with water
48 and CO₂ [4 - 6] without using any external stimulation, however, crack closure can reach
49 less than 0.18 mm. On the contrary, the cracks repaired autonomously usually incorporate
50 a specific healing agent within the matrix which varies in type and chemical-based
51 mechanism. Recently the possible addition of bacteria admixture, micro additives, micro-
52 grains, microcapsules, and nanomaterials without external intervention as the self-healing
53 agent has also been considered. Wiktor & Jonkers [7] and Nishiwaki et al. [8] reported that
54 incorporating the bacteria involves calcium carbonate as a biological precipitation of cracks
55 through the CO₂ reaction. Their research aimed to quantify the healing potential of two-bio-
56 chemical self-healing agent components embedded in expanded clay particles, acting as
57 reservoir particles and partially replacing coarse aggregate. These components are released
58 by crack ingress water and fill the cracks in the concrete mixture.

59 On the other hand, many researchers [9 - 15] investigated other methods for triggering
60 the healing agents (adhesives) whether embedded in capsule or vascular networks as the
61 mixing process. Nishiwaki et al. [8, 9] used a heating device that triggered parts of concrete
62 through pipes with a plastic organic film encapsulated by the repair agent which releases as
63 soon as it melts when heating filling the crack and hardening, recovering the strength of the
64 concrete mixture. Their concerns lie in the bacteria's survival within the concrete matrix as
65 the concrete process from the mixing and pouring environment might not be appropriate for
66 their survival with additional concerns about long-term survival through the life cycle of the
67 structure [8, 9]. Another study by Dry [10] reported the timing and location release of
68 sealants, adhesives, and waterproofing encapsulators placed internally to acquire the
69 durability required. Their results showed that some of these encapsulations may appear in
70 the fibers but could possess the chemicals where and when the matrix cracks, causing the fiber
71 to crack and release chemicals. Tittelboom et al. [11] explore the utilization of computed
72 tomography and visual observation of crack faces while using an encapsulated healing agent
73 embedded in the mortar matrix to obtain self-healing properties. Their results showed the cracks
74 filling with a healing agent and more than 50% of strength was recovered. Further, they reported
75 that the water permeability would reduce and hence the proposed autonomic technique can
76 resort partially to the concrete properties.

77 Joseph et al. [12] investigated the addition of adhesive-filled glass reservoirs as self-
78 healing agents on reinforced mortar beams subjected to two cycles of loading. The results
79 revealed that there was evidence of crack-healing following the first loading cycle and new
80 crack formation during the second loading cycle, in addition, to secondary healing for the new
81 secondary cracks. They were motivated to provide more data for the long term in terms of
82 numerical methods. Homma et al. [13] explain the utilization of three fibers (polyethylene (PE),
83 steel cord, and hybrid composites) to examine the self-healing properties fo fiber reinforced
84 cementitious composites (FRCC) through cracking using tension test and retained at 28 days
85 after water curing. Their results revealed that the PE fiber has provided the most influence based
86 on the volume in bridging the crack and crystallization products attached easily to the larger
87 numbers of PE fibers, in addition to the reduction in permeability coefficient that was achieved.
88 They observed the hydration degree has a slight influence on the self-healing capability.

89 Nishiwaki et al. [14] have examined other various types of synthetic fibers that have
90 different chemical properties such as polyvinyl alcohol (PVA), ethylene vinyl alcohol (EVOH),
91 polyacetal (POM), and polypropylene (PP) on FRCC evaluating the self-healing capability of
92 FRCC. Their microscopic results showed the fibers' polarity provided a bridging crack through
93 self-healing precipitation and filled the cracks, in addition, reduced the water permeability
94 coefficient and in some cases no water tightness recovery. Nevertheless, they ensured that the
95 chemical properties of the fibers and geometrical properties of the crack surface from
96 roughness, complexity, and continuity of the fibers influence the self-healing properties in
97 terms of water tightness. Mauser et al. [15] stated that the autogenous methods mainly depend
98 on mineral admixtures such as fly ash and fiber addition, such as polyvinyl alcohol (PVA)
99 fibers. Their investigation revealed that these additives have great potential for the self-
100 healing process in concrete and provide good results in real applications under certain curing
101 conditions. These fibers could help in enhancing self-healing through the process of
102 controlling the crack and accelerating CaCO_3 precipitation. Recent studies by Liang et al.
103 [16] and Hammad et al. [17] showed that these fibers (PVA) have provided high polarity
104 synthetic composite and act as a bridge through the crack [17].

105 Although the above-mentioned techniques are widely used, several researchers [18 – 21]
106 observed various challenges and limitations when applying mineral admixture and PVA
107 additives, utilizing the triggers and microcapsules systems. These challenges can be limited by
108 the chemical triggers existing within the solution and along the fibers including, pH values and
109 ions charge on the fiber surfaces. For instance, Dong et al. [18] established a microcapsule
110 system to contain the chemical self-healing for cementitious composites. The survival
111 challenges could be overcome by capsulation; however, it is required to hatch the healing
112 agent through activation of the healing process. Method of the EDTA (Ethylene Diamine
113 Tetra- acetic Acid) titration method was utilized to release the corrosion inhibitor healing
114 agent from the microcapsule covered by polystyrene resin (PS). This is functioned by time
115 and wall thickness of the microcapsule. Nevertheless, the corrosion inhibitor release rate is
116 noticeably influenced by the pH value which increases with the decreasing pH value, which
117 is a bit not controllable. On the other hand, Lv et al. [19] developed a polymeric
118 microcapsule type utilizing the phenol formaldehyde (PF) resin as a shell and
119 dicyclopentadiene (DCPD) as a healing agent for self-healing microcracks in cementitious
120 materials. Their results provided that the microcapsules have excellent stability in hatching
121 the microcapsules by crack trigger and releasing the healing agent in a stable manner healing
122 the cracks simultaneously, however, no rate or insurance that the microcapsules will survive
123 for the long term was explored or investigated. Xu et al. [20] used ultrasonic wave-induced
124 to trigger the microcapsules for healing agent release. They found that this method was
125 controllable and cost-effective. The results revealed the strength recovery for mixes
126 triggered by ultrasonic were 2 – 4 times higher than mechanical-triggered ones. Yet still it
127 is not manageable to trigger the healing agent by ultrasonic.

128 Consequently, although several trials were proposed to overcome the survival
129 problems using trigger additives, vessels, and microcapsules, other researchers [21, 22] have
130 suggested having the coupled effect using fibers and bacterial admixtures. Feng et al. [21]
131 investigated the utilization of hybrid techniques by using bacteria and fiber as it has the
132 potential to enable excellent self-healing performance in concrete. Their experimental
133 program studied the coupled effect of PP fiber, PVA fiber, and bacteria on the self-healing
134 efficiency of concrete. The results revealed that PP and PVA fiber would reduce the bacteria

135 concentration. The crack width of 300–500 μm was healed within specimens with bacteria
136 and fiber than that with bacteria only. Further, the water tightness and flexural strength
137 recovery were improved as a result of calcium leaching and calcium ions utilization
138 deposition on fiber surfaces. In addition, they found that the PVA fibers filled the cracks
139 with polarity groups and cell structure of polyvinyl alcohol fiber on calcium carbonate
140 nucleation. Furthermore, Qiu et al. [22] studied the inclusion of slag-based ECC as it has the
141 potential for autogenous healing. Several factors: slag content, crack width, and environmental
142 alkalinity, on the efficiency of the autogenous healing of ECC were explored. They observed that
143 the single-cracked ECC specimens with different slag content and crack width under conditioned
144 underwater or NaOH/dry cycles. The healing results revealed the coupling effects of crack width,
145 slag content, and alkalinity conditions. However, drawbacks such as limited maximum allowable
146 crack width which could be only partial or no healing. The CaCO_3 could be produced as the main
147 healing component under water/dry conditioning while the NaOH/dry cycles condition initiates
148 the slag hydration for 24 hours and results in the formation of C-S-H and CaCO_3 . It is concluded
149 that CaCO_3 precipitation is more effective in engaging autogenous healing than the formation of C-
150 S-H. The concept of associating allowable crack width and slag content is proposed, which would
151 guide ingredient selection and component tailoring to engage robust autogenous healing in ECC in
152 the future.

153 In the previous studies, the coupling effect of the two techniques autogenous and
154 autonomous has the potential to overcome many challenges instead of utilizing other
155 chemical additives or encapsulated systems. Yet still fewer researchers explored this
156 combination as mentioned earlier. Nevertheless, gaps remain not demonstrated on the
157 impact of the autonomous in comparison to autogenous self-healing in repairing the pre and
158 post-cracking of the damaged elements and the restoration of their mechanical properties.
159 Thus, this study explores the coupling effect utilizing bacteria, PVA fibers, and mineral
160 admixtures such as fly ash, observing the improved properties and self-healing capacity of
161 concrete in terms of mechanical properties restoration represented in compression and
162 flexural strength. In addition, it introduces the hybridization techniques of the two self-
163 healing techniques to stand on their impact in enhancing and restoring the compression and
164 flexural strength of the cube and prism specimen as a demonstration for further investigation
165 of structural elements under operation while managing to explore the durability
166 performance of the self-healed produced concrete using permeability and water absorption
167 tests.

168 2. Research Significance

169 Recent literature compares the results of the two available techniques: autonomic and
170 autogenous with other systems to trigger the healing agent whether through encapsulation
171 or vessel system. Usually, the aim is to overcome the many challenges from bacteria
172 survival or healing agent release on time and location of repairing the crack. Other
173 drawbacks involve the bacteria accommodation in the concrete mixture. The deposition of
174 CaCO_3 on the surface of the fiber made the possibility of achieving the location and timing
175 required by the bacteria with the contribution of mineral admixtures such as fly ash and
176 PVA fibers to bridge the crack and fill it. This potential motivates the study to explore more
177 about the pre and post-cracking of the concrete specimens within the mechanical properties
178 in terms of compressive and flexural strength at long aging. This action would ensure crack
179 closure and an impermeable concrete surface for absorbing hazards and deleterious

180 materials affecting the reinforcement with corrosion and other defects especially in the
181 coastal environment.

182 3. Experimental Program

183 3.1 Materials and Mix Design

184 3.1.1 Cement

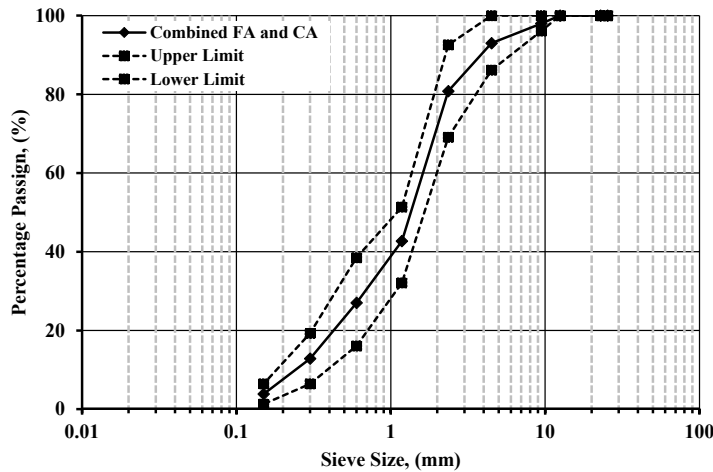
185 The cement used was Ordinary Portland Cement, grade 42.5 MPa (N/mm²). The cement's
186 properties are compatible with European standards EN 197 [23] and Egyptian standards
187 (4756-1 /2007) [24] as provided by the manufacturer. The physical, chemical, and
188 mechanical properties of the cement are described in Table 1.

189 3.1.2 Fly Ash

190 Fly ash class F originates from anthracite and bituminous coals. It consists mainly of
191 alumina and silica. Class F fly ash has a lower calcium content than Class C fly ash. The
192 rest of its chemical composition is presented in Table 1. The Additional chemical
193 requirements as per ASTM C 618 [25] are listed in Table 1.

194 3.1.3 Fine and Coarse Aggregate

195 Natural siliceous sand was used as fine aggregate, and crushed dolomite stone was used as
196 coarse aggregate. Fig. 1 shows the grain size distribution of combined fine and coarse
197 aggregates. As deduced from Fig. 1, the nominal aggregate size was 12.5 mm. The physical
198 and chemical properties of fine and coarse aggregates are also represented in Table 2.



199

200 Fig. 1. Sieve analysis of fine and coarse combined aggregate with limit ASTM C33[26]

201 The fine aggregate utilized silica sands for applications other than building because of their
202 high silica content (more than 95% SiO₂). Silica sands include a significant quantity of
203 quartz, abundant in silica, and, more importantly, relatively little clay, iron oxides, or
204 chromite, a refractory mineral. Their grain size distribution is typically restricted (0.1 to 2
205 mm).

Table 1. Physical, chemical, and mechanical properties

Chemical composition in (%)			
Component (%)	OPC	FA Class f	ASTM C 618 [25] Requirements (%)
SiO ₂	47.09	47.09	70
Al ₂ O ₃	17.41	17.41	70
Fe ₂ O ₃	8.34	8.34	70
CaO	13.98	13.98	-
MgO	1.85	1.85	-
SO ₃	4.65	4.65	-
Na ₂ O	2.44	2.44	-
K ₂ O	1.8	1.8	-
Loss ignition	2.2	1.79	-
Physical properties			
Density (kg/m ³)	3160	2150	-
Activity index % (after 28 days)	-	77.5	-
Activity index % (after 90 days)	-	85.6	-
Specific gravity	3.16	-	-
Initial setting time (min)	180	-	-
Soundness (mm)	1	1	-
Fineness %	-	22.43	-
Water Absorption (%)	32	-	-
loss of ignition (%)	2.2	-	6
Sulfate content (SO ₃) %	2.7	-	5
Blaine fineness (cm ² /g)	4100	2469	-
Reactive SiO ₂ %	-	40.34	-
Blaine (cm ² /g)	-	3330	-
Alkalis%	-	2.46	-
Free CaO	-	0.03	-
Color	Grey	Grey (blackish)	-
Compressive strength (MPa)			
Mechanical properties			
1 day	25	-	-
2 days	38	-	-
28 days	68	-	-

207

208 Table 2 shows the physical properties of the fine and coarse aggregate used in this
 209 investigation. Sieve analysis of the combined fine and coarse aggregate used in the mix
 210 design, as shown in Fig. 1. These properties were determined according to ASTM C 33[26],
 211 BS EN 933-1 [27], ASTM C117 [28], ASTM C127[29], ASTM C128 [30], BS 812-2[31],
 212 BS 812-103 [32].

213

Table 2. Physical and chemical properties of fine and coarse Aggregate

Physical and chemical properties		
Property	FA	CA
Specific gravity	2.62	2.65
Volume weight	1.84 MPa	1.73 MPa
Void ratio	31.0%	33.8%
Absorption percentile	1.6%	1%
Fineness modulus	6.62	2.72
Clay, silt, and dust ratio	0.09%	2.0%
Percent of chloride	0.03%	0.03%

214 **3.1.4 Polyvinyl Alcohol Fiber**

215 Polyvinyl alcohol (PVA) fiber has been used in the concrete mix as it has a very high
 216 elastic modulus and tensile strength. The properties of the fiber are listed, as shown in Table
 217 3.

218 **Table 3.** Physical and technical properties of PVA fiber

Content	PVA
Length	9 mm
Diameter	0.04 mm
Specific gravity	1.12
Elastic modulus	40 GPa
Tensile strength	1320 MPa
Modulus strength	34 (GPa)
Elongation at break	6.80 %

219 **3.1.5 Producing Bacteria and Bacterial Environment**

220 *B. subtilis* was selected based on ease of availability and quickly cultivated. The typed
 221 culture of *B. subtilis* (ATCC23857) is a soil-found strict aerobic gram-positive, rod-shaped
 222 bacteria that can withstand high temperatures and produce spores dormant for many years.
 223 Using the MacFarland standard, the fresh bacterium strain was standardized [33] to obtain
 224 108 cells/ml, which was used in this study as adopted by Tian et al.[33].

225 The bacteria were cultured and grown for the investigation using two culture mediums,
 226 NH₄-YE Nutrient Broth Medium and NH₄-YE Agar Plate Medium, besides the Tris buffer
 227 solution and other components like peptone, yeast extract, and ammonium sulfate, which
 228 create the medium of (NH₄SO₄). The tris buffer solution was created by 16.20 grams (g) of
 229 tris (hydroxyl methyl amino meth) dissolved in about 0.5 liters (L) of distilled water to
 230 create a colorless solution that was used to create 1 liter (L) of tris buffer solution. A pH of
 231 9.0 was achieved by titrating the solution with 1 molar hydrochloric acid (HCl). The
 232 remaining volume of 1 L was then filled with distilled water. The NH₄-YE Nutrient Broth
 233 Medium was created with 20 grams of yeast extract and 10 grams of NH₄SO₄ added to one
 234 liter of tris buffer solution in a conical flask. The mixture was then thoroughly agitated until
 235 the yeast extract was dissolved. Before inoculating the test organism, the solution was
 236 autoclaved according to the usual protocol at 121 °C for 15 min. It was then allowed to cool
 237 to room temperature (25 °C). Some species generate the enzyme urease, which degrades

238 urea to create ammonia [2, 14, 34, 35]. The motility and indole confirmed the identity of the
239 isolate, and urease (MIU) biochemical assays were used to validate the identification of the
240 bacteria, as reported by Feng et al. [21].

241 Finally, a microscopic confirmation of the production of calcium carbonate residue was
242 confirmed after verifying the organism's motility, indole, and urease identities using the
243 MIU (Motility Indole Urea) test. Then, Microscopic analysis revealed the organism's
244 capacity to precipitate calcium carbonate. $\text{CaCl}_2\text{H}_2\text{O}$ and urea (3 g in 100 ml of sterile
245 distilled water) were added to the nutritional solution after sterilizing it for 15 minutes at
246 121°C [2, 21]. After allowing it to cool, the organism was injected into it. Following seven
247 days of interval incubation at the optimum temperature and pH on days 0, 7, 14, 21, and 28
248 on an orbital shaker, this was then studied under a microscope. The precipitation of CaCO_3
249 by the organisms following it, which was Gram's stained and observed under the
250 microscope, demonstrated the precipitation of calcium carbonate.

251 After that, a nutrient broth medium was used to subculture the *B. subtilis* strain. The
252 medium was serially diluted to provide 10^8 cells/ml before being introduced using a sterile
253 loop from the Petri plate holding the organism. The nutrient broth was injected in a ratio of
254 1:10 into a 250 ml conical flask that contained 200 ml of the sterile culture medium and was
255 then covered with cotton wool and aluminum foil to prevent contamination. The culture
256 media were incubated at 30°C and then moved to an orbital shaker at 130-300 revolutions
257 per minute (rpm) for 10 days to ensure the maximum growth of the bacteria.

258 The test isolates and preserves the pure culture of *B. subtilis*, initially kept on nutrient
259 agar slants, producing uneven, dry, white colonies. Before inoculating into the prepared
260 medium, it was subculture regularly to get new culture. The culture procedure was carried
261 out in a sterile environment [2]. Fig.2 depicts the prepared 250 ml medium (Nutrient broth)
262 before autoclaving and the cultivated bacteria solution following shaking.



263 **Fig. 2. Bacterial solution**

264 **3.2 Concrete mix design**

265 The concrete mixes were designed through the ACI 211.1-91 [36], including six mixes
266 containing bacteria, and PVA fiber added while having a control mix without any additional
267 minerals or admixtures for comparison purposes. Three of the six mixes include PVA fibers
268 at different volume percentiles ranging from 1 to 2%, while the sixth mix combines PVA
269 fiber and bacteria. The other two mixes; one represents the use of OPC as control and the

270 other uses bacteria only. Tables 1, 2, and 3 show the physical properties of cement, fly ash,
 271 PVA fiber, and fine and coarse aggregate used for mix design. Table 4 presents the concrete
 272 mix design for a one-meter cube. The target strength of the concrete was C32 grade and the
 273 water-to-cement ratio of 0.43 for preparing the specimens. The following specimens were
 274 prepared for each test variable; 126 cubes of side dimensions of 150 mm and 108 prisms
 275 dimensioned 100 x 100 x 500 mm. The six mixtures include one control mix, one bacterial
 276 mix, three PVA mixes at different percentiles, and one combined mix, bacterial with PVA
 277 at 1.0% by volume fraction (VF). As shown in Table 4, the control mix was denoted by
 278 “OC,” while “BC denoted the bacterial concrete mix. In addition, those with PVA were
 279 denoted by “PVAC”. While the “1” indicates the percentile of PVA fiber added. For
 280 instance, “1” means 1 percent of PVA volume fraction was added, while “1.5” and “2”
 281 stands for 1.5 and 2 percent of PVA volume fraction. Only the sixth mix was represented
 282 by “BC+PVAC1,” which combines bacterial and PVA fiber of VF of 1.0%. The selection
 283 of the volume fraction of PVA was based on the study carried out by Srinivasa et al. [37].
 284 The study investigated the utilization of PVA from 0 to 2% through collected data from
 285 literature and found that the results are more reliable when using PVA volume fraction
 286 ranges between 1 to 2%, in addition, it provides an enhancement to compressive and tensile
 287 strength. Based on this research, it was deduced that the suitable PVA volume fraction
 288 would be between 1 to 2%, hence, three PVA volume fraction was selected, 1, 1.5, and 2%.
 289

Table 4. Details of concrete mix design

ID	Water, liter /m ³	Cement content, kg/m ³	Fly Ash, kg/m ³	Fine Aggregate, kg/m ³	Coarse Aggregate, kg/m ³	Bacteria	PVA Addition (%) by volume
OC	172	400	120	550	1165	---	---
BC	172	400	120	550	1165	Count of 1.08*10 ⁸ cells/ml, solution concentration of 600 nm/liter	---
PVAC1	172	400	120	550	1165	---	1%
PVAC1.5	172	400	120	550	1165	---	1.50%
PVAC2	172	400	120	550	1165	---	2%
BC+ PVAC1*	172	400	120	550	1165	Count of 1.08*10 ⁸ cells/ml, solution concentration of 600 nm/liter	1.0%

290 *The PVA fiber Volume fraction was elected based on the optimized values in terms of workability and hardening
 291 properties of mixes with PVA fiber volume fraction mixes; PVAC1, PVAC2, and PVAC3.

292 3.3 Mixing Process

293 The study's objective is to observe the influence of two mechanisms, autonomic and
 294 autogenous methods, for healing the cracked concrete and developing its strength and other
 295 durability properties. In addition, the influence of replacing cement with binding materials
 296 such as fly ash on autogenous self-healing and closure of the cracks. A further combination
 297 of the two mechanisms was considered and their influences on crack closure were reported

298 as shown later in Fig. 3, 8, and 10. This objective was extended to observe the influence of
299 combining the two mechanisms on the closure of concrete cracking as well.

300 The concrete mixtures were produced following the procedures outlined by Zhou et
301 al.[38]. Zhou et al.[38] adopted the sequence of adding dry components from cement and
302 fly ash first together while mixing for 2 minutes at low speed (600 rpm) in the electric
303 concrete mixer. Then, an appropriate solids amount (2/3 of the total volume) was mixed
304 with half of the calculated mixing water for 2 minutes at low speed. the fine aggregate (sand)
305 was, then added incrementally over 1 minute while continuing to mix at low speed. The
306 mixture was mixed for an additional 2 minutes after the full addition of sand. The PVA
307 fibers were slowly added over 1 minute at low speed. The mixture was left to sit undisturbed
308 for 1 minute without mixing. Then mix at high speed (4000 rpm) for 2 minutes to uniformly
309 distribute the fibers. The remaining mixing water was incrementally added over 1 minute at
310 low speed. The final mixing was conducted at high speed for 2 minutes to produce a
311 homogenous mixture. In the case of mixtures including bacteria, the calculated bacterial
312 solution was injected into the continuously mixing concrete using an injection device. This
313 ensured thorough dispersion of the bacteria throughout the mixture.

314 3.4 Sample Preparation

315 A total of 126 cube specimens and 108 prism specimens were prepared by pouring the
316 concrete mixes into the molds; then, the specimens were placed onto the vibrating table,
317 ensuring the compaction of the concrete thoroughly. The specimens were left in the molds
318 of the laboratory for 24 hours. Then, the specimens were removed from the molds and
319 placed inside curing tanks for 7, 28, and 56 days until testing. All samples were prepared,
320 and water cured by BS EN 12390-2 [39].

321 3.5 Details of Test Specimens

322 The experimental program contained four main variables representing different
323 mixtures, including varied ratios of PVA fibers volume (1.0, 1.5%, and 2.0%), adding the
324 bacterial solution to the mixing water with a count of 1.08×10^8 cells/ml (solution
325 concentration of 600 nm/liter) and ordinary concrete as a reference mix. The experimental
326 program comprised 9 cube specimens for each mix and the cracking load was assigned
327 accordingly to the control mix. The specimens covered the ages of 7, 28, and 56 days.
328 Similarly, 3 scaled prisms of span 500 mm, depth 100 mm, and width 100 mm were
329 encountered for each mix at two different ages, 28 and 56 days. 18 cubes were disturbed as
330 follows for each durability test: sorptivity, absorption, and permeability at 7, and 28 days of
331 age.

332 For assessing the gain and recovery of compressive and flexural strengths, each mix has
333 at least 6 cube specimens at 7, 28, and 56 days of age. Three of the specimens were
334 undamaged and the other was pre-damaged at about 60%. Then, the specimens are exposed
335 to the healing process. The process of healing acts after cracking the specimens with an
336 initial cracking load. The healing process adopted was wet and dry cycles of curing to assess
337 the regain after the healing process through testing again. The duration of curing through
338 the wet and dry cycle healing process is 28 and 56 days of age. It should be mentioned that
339 only those specimens that were pre-damaged at 7 days of curing were exposed to a healing

340 process of 28 days. The others ages: 28 and 56 days were exposed to the healing process at
341 the same curing ages; 28 and 56 days as well.

342 **3.6 Test Methods**

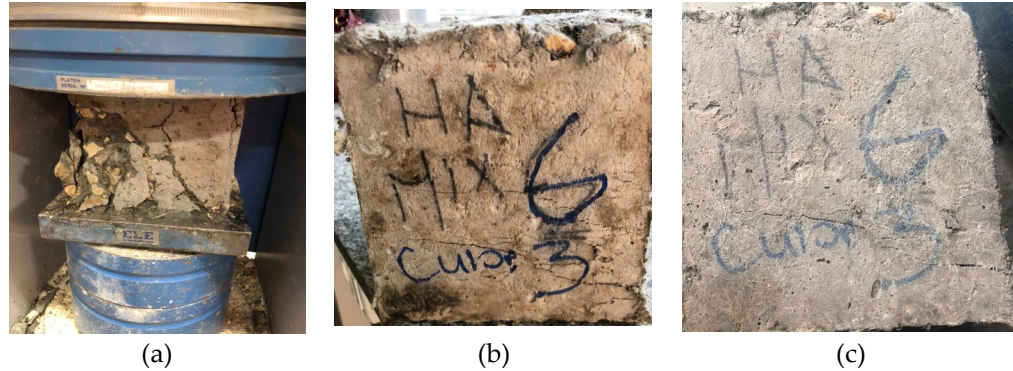
343 Several tests were conducted to determine the fresh and hardened state properties of the
344 produced concrete. In addition, various durability tests were carried out to assess the
345 durability of the concrete with PVA or bacteria. Slump tests for the fresh concrete mixes
346 were carried out to determine the workability of the fresh concrete mixes and were
347 conducted as per ASTM C143 / C143M [40]. Slump tests are used to measure the vertical
348 settlement or "slump" of a standardized sample, which starts by filling with concrete the
349 frustum cone into layers. Each layer was tamped 25 times then the mold was removed and
350 inverted, allowing the sample to subside under its weight for 3 minutes. The slump is
351 measured as the difference between the original height and the final settled height of the
352 sample. The slump value indicates the concrete's consistency and flowability, with a higher
353 slump indicating higher workability.

354 The density of the hardened concrete was conducted according to ASTM C642 [41] at
355 the age of 28 days. In this test, the hardened concrete sample is weighed after an oven-dry
356 at a temperature of 100 to 110 °C for not less than 24 hours allowing it to cool in dry air.
357 Then the sample is weighed after being immersed in water at approximately 21 °C for not
358 less than 48 h. Finally, the sample is placed and covered with tap water boiled for 5 h. Then
359 the sample is allowed to cool down not less than 14 h reaching room temperature of 20 to
360 25 °C. The steps should be repeated at each stage until the difference between any two
361 successive measurements is less than 0.5 % of the lowest mass obtained in the case of oven-
362 dry and observed an increase in mass less than 0.5% of the larger mass provided in case of
363 water saturation. The bulk density can be calculated through the equations provided by
364 ASTM C642 [41] for oven-dry, immersed, and boiling cases

365 The compressive strength test measures the maximum load a concrete sample, whether
366 cylindrical or cube, can bear before failure when loaded axially in compression. The
367 compressive strength at a given age is evaluated by calculating the average strength of three
368 consecutive samples. This test is carried out to determine the loading capacity of hardened
369 concrete. However, in this study, the compressive strength was measured in two stages. The
370 first stages included testing the control specimens till failure. Thus, the peak load can be
371 known from the very beginning, at 7, 28, and 56 days. The second stage relies on the pre-
372 damaged three specimens up to 60% of the peak compressive strength of the un-damaged
373 specimens, or the corresponding load that produces a 0.1 mm crack width threshold or more
374 [33, 42 - 44]. This pre-damaging load level ensured visible cracking was produced to initiate
375 damage while avoiding complete crushing or pulverization of the samples. After initiating
376 cracks at the pre-determined cracking load level, the three pre-damaged specimens were
377 then exposed to wet and dry cycle curing methods at 7, 28, and 56 days depending on pre-
378 damage age to allow for self-healing [33, 42 - 44]. The cracked and healed strength obtained
379 after the curing periods was then used to evaluate the concrete mixtures' inherent healing
380 capabilities over time at different damage levels and curing durations through compression

381 testing till failure or crushing of the specimen. This testing methodology provided a
382 standardized approach to deliberately damage samples for quantification of self-healing
383 performance. Thus, there were two stages: one un-damaged and pre-damaging three
384 specimens for each mix at each age, as shown in Fig. 3-a and b.

385



386 Fig.3 Typical cube specimen (a) after failure (control/un-damaged specimen), (b) after pre-damaged by
387 60% of the ultimate capacity, and (c) after healing process exposure as per the age assigned for testing
388 till crushing failure.

389 It should be mentioned that the values reported were averaged from the three specimens
390 tested. As shown in Fig. 3-a, a typical control/un-damaged cube specimen was loaded till
391 achieving failure load then a similar cube specimen was loaded till reaching the cracking
392 load, as in Fig. 3-b. The cube specimen was cured by applying the healing scheme according
393 to the assigned age and prepared for testing to failure, as shown in Fig. 3-c. It should be
394 mentioned that the undamaged and pre-damaged cube specimens were tested for
395 compressive strength as per BS EN 12390-3 [45] where the specimens were loaded at a
396 pacing rate of 240 kg/cm² per minute till the specimen failure using the universal testing
397 machine of capacity 2000 kN.

398 Similarly, the same loading scheme was followed for prism specimens to evaluate the
399 flexural strength of the specimen, whether undamaged, pre-damaged, or after exposure to
400 the healing scheme. The flexural test was handled for the control prism specimen to
401 determine the peak load as per ASTM C78/C78M [46]. The specimens were tested on the
402 flexural machine under two-point loading after adjusting a pacing rate of 24 kg/cm² per
403 minute till failure. Following the similar scheme of cube specimens, the prism specimens
404 were loaded till failure for control/un-damaged prism specimens, as shown in Fig. 4-a. 60
405 percent of the peak flexural load [47 - 49] or the corresponding load for the threshold crack
406 width of 0.1 mm was applied to the pre-damaged the prism specimen, see Fig. 4-b.
407 Thereafter, the specimens were left for curing as per the aging assigned for testing, as shown
408 in Fig. 4-c.

409 The curing regime in which both cube or prism specimens are cyclic wet and dry. The
410 curing process involves submerging the specimens into the water tank and drying them in
411 the air at room temperature, inside the laboratory. The process was repeated successively at
412 24-hour intervals. This method simulates natural environmental moisture fluctuations that
413 can trigger self-healing in cementitious materials as suggested by Yang et al. [50]. The
414 strength recovery was calculated as the percentage increase in peak load from the post-
415 cracking to the post-healing state. During testing, the crack behaviour under loading was

416 also observed. Additionally, surface cracks were observed before and after healing using a
417 visual inspection to make sure that the cracks were sealed. It should be noted that before
418 pre-damaging the cube or prism specimens, the specimens were water-cured until they
419 reached the age assigned for pre-damaging.



420 **Fig. 4.** Typical prism specimen (a) after failure, (b) after pre-damaged by 60% of the
421 ultimate capacity, and (c) after healing process exposure as per the age assigned for testing
422 till failure.

423 4. Experimental Results and Discussion

424 4.1 Slump

425 The slump was tested after putting all the concrete ingredients and mixing them to
426 determine the workability of the concrete after adding PVA fiber or the bacteria as per the
427 mix design. The results showed that the addition of both would reduce workability to a high
428 level. The mix OC, which represents the control provided a slump of 10 cm. However, when
429 adding the bacteria, as in mix BC, the slump reached 0.7 cm which means that the reduction
430 has reached 93% while the slump was reduced more than that by 95% when adding a VF of
431 1% PVA fiber as in mix PVAC1. The slump for mix PVAC1 was 0.5 cm. Similarly, mixes
432 PVAC1.5 and PVAC2 were reduced by 97 and 98% when the VF of the PVA fiber added
433 was 1.5 and 2%. When combining both bacteria and PVA fiber (mix BC+PVAC1), the
434 slump reached 0 cm which is a total reduction of 100%. From the results, the slump is
435 influenced by the addition of bacteria and PVA fiber although the replacement of fly ash
436 with cement should enhance the workability. However, fly ash did not counteract the
437 negative impact caused by the bacteria and PVA fiber interactions between additives that
438 dilute cement paste continuity. The spherical surface of fly ash would be the reason for
439 improving the workability or reducing water which was already considered while designing.

440 Topiča et al. [51] have studied the influence of PVA on cement paste in terms of fresh
441 and hardened properties. The results of the flow test revealed that increasing the addition of
442 PVA reduces the slump and workability as agreed with the investigation carried out herein.
443 Topiča et al. [51] suggested that this was due to the viscosity accompanied by the PVA
444 fibers which cause mixing and pouring problems. Hence, increasing the PVA content would
445 increase this viscosity and reduce the slump. Nevertheless, Topiča et al. [51] suggested a
446 hypothesis that required further investigation related to the relationship between the initial
447 and final setting time delay that occurs when using the PVA fiber and hydration process.
448 With their observation of setting times while flow and fresh state it was hypothetically
449 assumed that there might be an unusual bump resulting from the restored unhydrated C_3A
450 restored by the PVA barrier around the cement grains. These restored hydrated particles of

451 C₃A produce ettringite and thus increase the diffusion of the water to complete the hydration
452 of C₃A. Another aspect would be the bacteria itself which also showed a reduction in the
453 workability of the mixture BC and BC+PVAC1. This could be attributed to the absorption
454 of the bacteria for more water to deposit layers of CaCO₃ into the cavities, pores, and micro-
455 cracks of concrete [52]. Hence, their hydrophilic nature would reduce the water content
456 within the mix. Similar findings were deduced by Zhang et al. [53]. Their results provided
457 that the PVA fibers addition in cementitious composite decreased its workability.

458 The workability reduction increased from 60 to 30 mm with increasing the PVA volume
459 fraction (0.3–1.2%). Zhang et al. [53] attributed this behaviour to the creation of a network
460 structure by the PVA fibers within the cementitious composite. This action restrained
461 segregation and workability from being possessed. Further, they assumed that some cement
462 particles might be absorbed onto the fiber surfaces and wrapped the fibers around. This
463 behaviour would reduce the effective paste to contribute to the mixture's workability. It
464 should be noted that Zhang et al. [53] added a water reducer to their cementitious mixture
465 which was not countable here in this study as might influence the bacteria environment that
466 was not clarified in any existing literature review. On the other hand, Safiuddin et al. [54]
467 ensured that the bacteria would increase the workability and the enhancement may reach
468 45% higher than that of the control mix at high bacteria dosage. This was different from the
469 findings attained here in this study as the slump was reduced when using the bacteria (mix
470 BC). It should be mentioned that similar bacteria in Safiuddin et al. [54] investigation used;
471 the bacteria *Bacillus subtilis*. Although the enhancement observed by Safiuddin et al. [54],
472 stated that the bacteria activated once it encountered water, feeding on calcium lactate and
473 growing to self-heal the cracks at 48 hours increased to 72 hours at high bacteria dosage.
474 This action contradicted the slump results as this observation would absorb the water from
475 the fresh state. This is simply because the bacteria dosage was added at the mixing stage
476 without incorporating it within capsules. Further, an investigation is required in this area for
477 more clarification and demonstration of the influence of the bacteria on self-healing.

478 Hence, the findings confirm the need to use superplasticizers when using bacteria and
479 PVA fiber after exploring the influence of the superplasticizer on the performance of
480 bacteria and PVA fiber in the healing process of concrete. Superplasticizers achieve this
481 through their dispersive properties through electrostatic repulsion as dominant [55]. Flatt et
482 al. [55] stated that the superplasticizers in their basic forms such as sulfonated formaldehyde
483 condensate (SNFC), lignosulfonates, or salts of polycarboxylic acids (PCA) require
484 specified calculations related to steric repulsion. This dispersive effect increases the fluidity
485 of the cement paste, making it easier to uniformly disperse the hydrated cement, bacteria,
486 and fibers throughout the mix [52, 54]. Thus, such behaviour could counterbalance the
487 water-demanding nature of bacteria and the viscosifying effects of fibers, lubricating the
488 concrete matrix, untangling clumps, and preventing re-agglomeration during mixing. The
489 enhanced dispersion allows bacteria and fibers to be more equally coated by a hydrated
490 cement paste, reducing frictional interactions that enhance the workability. Hussein et al.
491 [52] have examined the suitable dosage of superplasticizer in their cementitious mixture
492 through different percentiles. They found that as the superplasticizer increased the reduction
493 of water content would reduce reaching 35% at 2.5 liters to each 100 kg cement and reducing
494 the water ratio from 0.42 to 0.27.

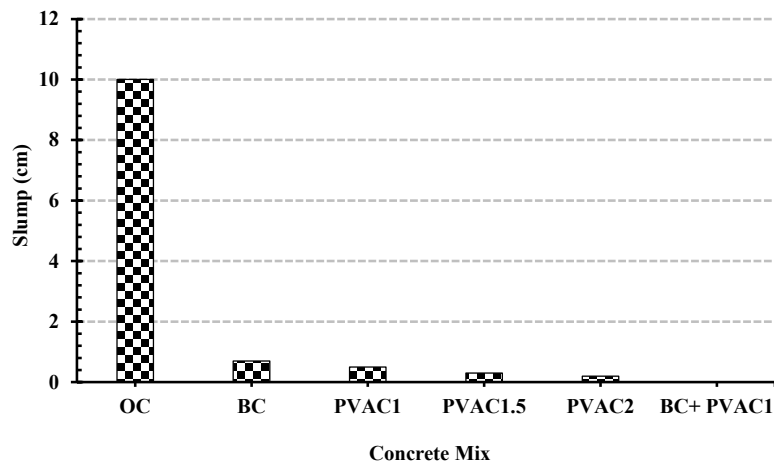


Fig. 5. Slump results for all mixes before hardening state properties.

495

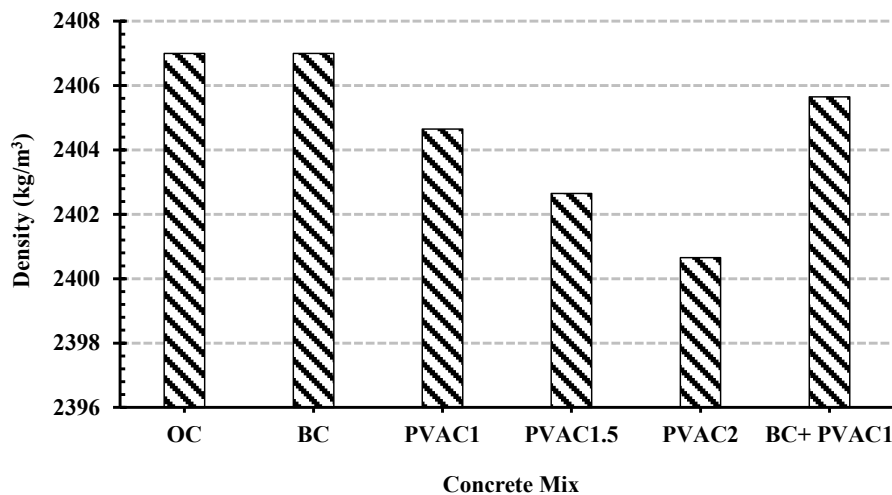
496

497 4.2 Density

498 The density of all mixes was measured from the cube specimens in their hardened state
 499 before implementing any healing process or pre-damaging to the cube specimen at 28 days
 500 of age. As shown in Fig. 6, the density at 28 days of age after hardening decreased slightly
 501 with the addition of PVA fiber. The density is an important aspect as it forecasts
 502 compressive strength and shows the possibility of the presence of pores or not as the
 503 relationship between the density and compressive strength is proportional [56]. In other
 504 words, as the density of the concrete mixture increases the compressive strength increases
 505 [56]. Nevertheless, very few researchers addressed the influence of adding PVA onto the
 506 mortar or concrete mixture. However, most of those exploring the self-healing techniques
 507 using the fly ash as partial cement replacement and PVA fiber did not investigate the density
 508 of the mixture produced either before or after the implementation of the healing process as
 509 scanned through the existing literature review [21, 22]. It is anticipated that the fiber would
 510 increase voids based on the investigation carried out by Topič et al. [51]. They reported that
 511 the addition of PVA into the cementitious matrix has increased the porosity and therefore
 512 reduced the density which in turn reduced the compressive strength of their mixture. This
 513 behaviour was observed using optical and electron microscopy images (SEM) [51].

514 Yew et al. [57] also explored the low volume fraction of PVA in a cement matrix and
 515 found that the PVA attains lower density in both light weight and normal concrete. They
 516 attributed this behaviour to lower specific gravity although Shafigh et al. [58] reported that
 517 steel fibers which is the most used fiber for improving the mechanical properties of concrete.
 518 Their results, contrary to the PVA fiber, revealed that increasing the volume fraction of steel
 519 fibers would increase the density of the concrete. Hence, Yew et al. [57] confirm that the
 520 low specific gravity would be the main reason for the slight reduction in density while
 521 increasing the PVA fiber volume fraction. However, when exposed to their concrete to
 522 preheating, the results revealed that PVA fiber tends to displace mortar in concrete. From
 523 Fig. 6, the mixes already included the bacteria besides the PVA fibers at different
 524 percentiles. As clear, the reduction in density is relevant to the addition of PVA fiber which
 525 agrees with the findings of Topič et al. [51] and Yew et al. [57]. As the PVA fiber percentile

526 increases the density decreases due to the lower specific gravity which is near to one as
527 addressed in Table 3.



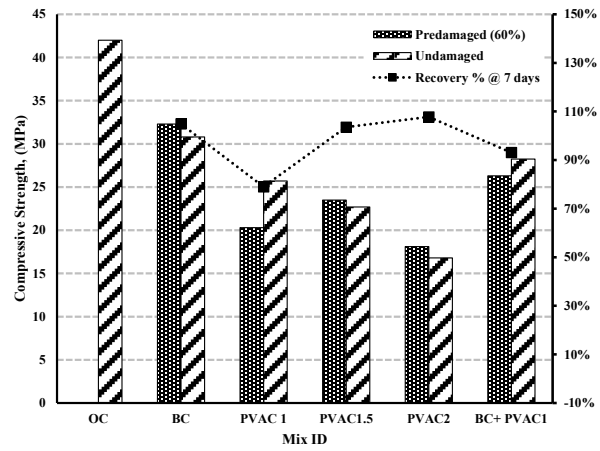
528
529 Fig. 6. Density results for all mixes at 28 days of age after hardening state properties
530 before initiating cracks or applying the healing process.

531 4.3 Compressive strength

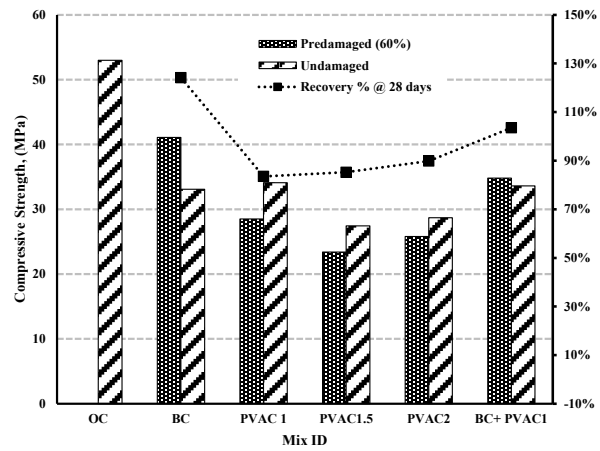
532 Compressive strength is a very important aspect of any structural element as concrete
533 can handle compression stresses more than tensile ones. Thus, concrete deterioration and
534 degradation of strength is a crucial issue. The healing and recovery of strength could provide
535 a new era in concrete technology especially when it comes to the repair and maintenance of
536 structures and their operation. Self-healing in this case could be an alternative even though
537 the capital of investment would be high at the beginning. From Fig, 7, both techniques of
538 self-healing enhanced and improved the concrete strength after being cracked. The figure
539 shows gained strength through the ages while initiating cracking through pre-damaged
540 specimens and the recovery gained after applying the healing process of a wet and dry cycle
541 for each mix with a period according to their ages except for 7 days of age, the healing
542 process of cycles wet and dry was applied for 28 days only. The initiation of cracking took
543 place after testing three specimens till failure (un-damaged) and the damaged specimens
544 were created for each mix by applying 60% of its capacity to initiate the crack width of
545 more than 0.1 mm. Fig. 8 shows the crack initiation of the cube specimens before and after
546 encountering the healing process.

547 Usually, the influence of the healing process can be evaluated through the crack closure,
548 as shown in Fig.8, and the compressive strength recovery was plotted as presented in Fig. 7
549 [59]. Zhang et al. [59] stated that the concrete itself cannot heal on its own as the hydration
550 reaction of cement particles and the crystallinity of additives is unable to close cracks of this
551 size. The evidence was deduced when leaving the initiated cracked cube specimen after 28
552 days of curing at room temperature. On the other hand, the self-healing granules provided
553 closure for the crack as stated by Zhang et al.[59] where their results revealed that at 7 days
554 of curing 0.963 mm would be repaired in just 7 days. However, it should be mentioned that

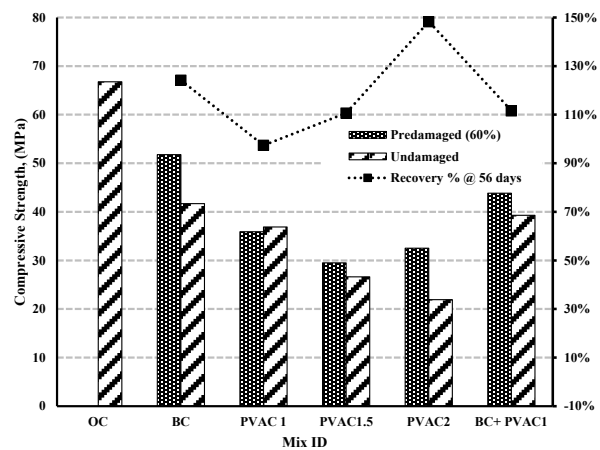
555 the faster healing process is dependent on the types of healing material used whether it is
 556 bacteria or chemical additives.



(a) 7 days*



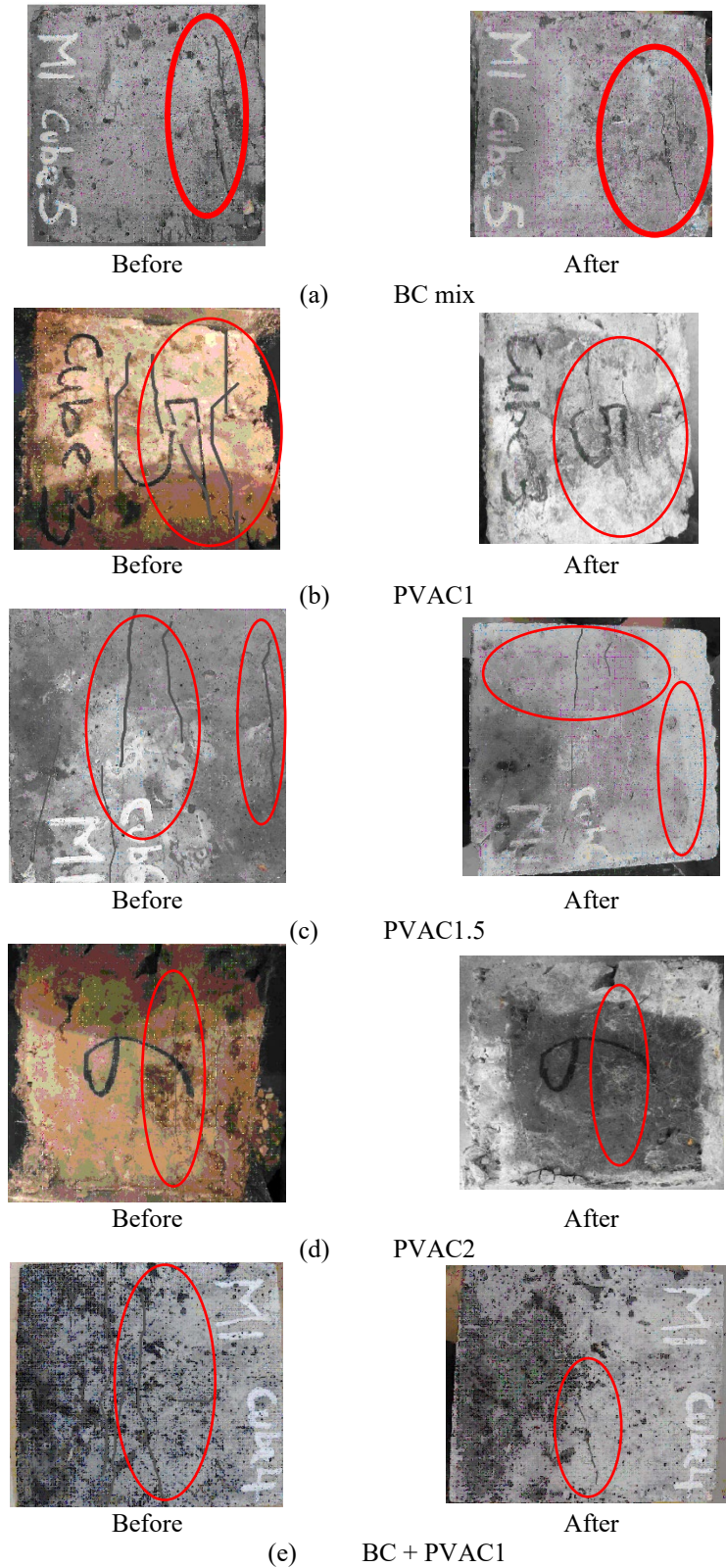
(b) 28 days



(c) 56 days

*The 7 days of age curing was then encountered in the healing process (dry and wet cycle) for 28 days

557 Fig. 7. Compressive strength results for the cube specimens for all mixes after hardening
558 with (pre-damaged) and without (undamaged) applying the healing process at (a) 7, (b) 28,
559 and (c) 56 days of age.



560 Fig. 8. Crack closure of cube specimens at initiating cracks and after applying the healing
561 process at 28 days of age for mix (a) BC, (b) PVAC1, (c) PVAC1.5, (d) PVAC2, and (e)
562 BC + PVAC1

563 In Zhang's study, the materials were self-healing granules, which require no temperature
564 or chemical activation and the inner core of the inorganic mineral of these granules provides
565 good compatibility and long-term stability with cement-based materials [79]. Nevertheless,
566 the healing bacteria used and PVA fiber including the use of fly as mineral additives helped
567 in healing the concrete, as shown in Fig.8. Compared with the control mix, it is clear from
568 Fig. 7-a, b, and c, that the undamaged specimens attain a value of 73, 62 and 62% for mix
569 BC of that of the control mix at 7, 28 and 56 days of age. Similarly, the mixes PVAC1,
570 PVAC1.5, and PVAC2 revealed a compressive strength for the undamaged cube specimen
571 of 61, 64, 55, 54, 40, 40, 54, and 33% at 7, 28 and 56 days of age, respectively. while the
572 compressive strength of undamaged cube specimens for mix BC+PVAC1 showed values of
573 67, 63, and 59% of that of the control mix, at 7, 28, and 56 days, respectively. It should be
574 noticed that the crack widths were not measured as the crack pattern was different than the
575 flexural, as shown in Fig.8.

576 From Fig.7, the compressive strength of cube specimens for BC mix at 7 days has a
577 recovery of 105% after the healing process. While those with added PVA fiber at 1, 1.5, and
578 2% the recovery at 7 days were 79, 104, and 108%, respectively for mix PVAC1, PVAC1.5,
579 and PVAC2. The mix BC + PVA 1 was recovered by 93%. Thus, the PVAC2 provided the
580 highest compressive strength recovery which is attributed to the lower compressive strength
581 of the un-damaged cube specimens due to the high PVA volume fraction. This high volume
582 fraction of PVA fiber increased the porosity, which in turn lowered the compressive
583 strength. Also, it should be mentioned that the OC mix might have provided a greater grade
584 at failure stress than other mixes with BC and PVA addition at 7 days of age.

585 At 28 days, the recovery revealed a different trend than that of 7 days. The mix BC
586 provided a strength recovery of 124 %, while the mix PVAC1, 1.5, and 2 provided a
587 recovery of 84, 85, and 90%, respectively. Finally, the mix BC + PVAC1 showed a strength
588 recovery of 104%.

589 At 56 days, the recovery revealed a similar trend with lower gaining strength. The mix
590 BC revealed a strength recovery of 124%, while the mix PVAC1, 1.5, and 2 retained a
591 strength of 97, 111, and 148%, respectively. However, the mix BC + PVAC1 showed a
592 strength recovery of 112% which is between that of mix BC and mix PVAC1 individually.
593 The mix BC and PVAC2 showed improvement relative to those with mix BC + PVAC1.
594 The reason for the improvement in general along with those of coupled effect was explained
595 by demonstrating the mechanism of using bacteria or PVA fiber or utilizing both combines.
596 In general, lowering the PVA fiber would reduce the porosity and therefore would increase
597 the compressive strength. As clarified earlier through ages, the un-damaged cube specimens
598 for mix PVAC1 were relatively higher than those of the mix PVAC2, which confirms the
599 existence of more voids and lower density [51, 56, 57] as explained earlier in section 4.2.
600 this behaviour would, in turn, reduce the compressive strength of the concrete mixture
601 regardless of the bridging provided by the PVA fibers and the precipitation of high calcium
602 carbonate that would enhance the concrete performance and fill the voids as explained in
603 the next few lines through the studies reported by Feng et al. [21] and Qiu et al. [22].

604 The mechanism of both bacteria and PVA fiber was reported by Feng et al. [21]. Feng
605 et al. [21] observed the presence of a high concentration of nutrients and some intermediate
606 metabolite or inducible enzyme in inoculated bacterial solution. The growth rate of the
607 bacteria decreased with the greater consumption of intermediate metabolite and hence
608 induced enzymes could be developed through the anabolic process of bacteria. The
609 reduction in the growth rate of bacteria was measured by breeding speed and the death rate
610 occurred through metabolite accumulation. However, the results revealed that calcium
611 carbonate possessed in a solution even with different fiber types was all calcite.
612 Nevertheless, both PP and PVA fiber showed no significant influence on the components
613 of products induced by bacteria [21]. Through their XRD, it could be observed that an
614 increase in peak intensity occurs with the inclusion of fiber into the solution and PVA
615 showed higher angles which implies the formation of larger and smaller crystallites [21].
616 Through their investigation, the particle size was measured to evaluate the volume fraction
617 of calcium carbonate precipitation by PVA fiber, which showed a higher amount of larger
618 particle size of calcium carbonate precipitation. In other words, the PVA presence did not
619 influence the polymorph of calcium carbonate induced by bacteria, but PVA fiber increased
620 the particle size of calcium carbonate [21].

621 The coupled effect of PVA fiber and bacteria was observed when Feng et al. [21]
622 observed white crystals precipitated on the fiber surface of the specimens containing BC
623 and PVA fiber more than those of PVA fiber only. The main elements of the precipitation
624 were C, O, and Ca, confirming the deposition particles were calcium carbonate. In addition,
625 microbial-induced calcium carbonate absorbed on the surface of cracks was observed. They
626 attributed that the contribution of PVA would be due to the high polarity strength in their
627 molecular structures which easily attract the calcium ions and promote the formation of
628 calcium carbonate, in addition to, their analysis of the cell parameter which provided close
629 results to those of calcite which means that the hydroxyl groups of crystalline PVA are
630 almost equal to that calcium ion of aragonite, generating aragonite requires a large number
631 of magnesium ions or special proteins that are rare inside the paste matrix [21]. Hence, both
632 bacteria and PVA possess nucleation sites for calcium carbonate, inducing calcium
633 carbonate precipitation, which was explained by the high utilization of calcium ions in
634 specimens including bacteria and PVA fiber, in addition to, the difference in particle size
635 for calcite generated in solution for mixes including PVA fiber than those with bacteria
636 only.

637 On the other hand, Qiu et al. [22] observed the mechanism of PVA fiber with other
638 mineral admixtures such as the slag, and deduced that the healing products, distinct from
639 the matrix, grew in the crack and almost filled the 100 μm gap. The healing products are
640 composed of irregularly precipitated crystal-like particles. While the large particles (\geq
641 $10\mu\text{m}$) fill the major portion of the gap, smaller particles ($\leq 10\mu\text{m}$) can be found in the void
642 between the large particles and the crack surface. the crystal-like particles grow from very
643 small precipitates, several hundreds of nanometers in size, and precipitate on the PVA fiber.
644 Fiber bridging might very likely facilitate the precipitation of healing products and promote
645 healing in Engineering cementitious concrete (ECC). Through the EDX, the healing
646 products composition was identified and were as follows; calcium, silicon, and carbon
647 possess the presence of CaCO_3 and/or C-S-H as the main products, in addition, the Ca/Si
648 ratio of the healing products for the samples was in the range of 5.63 to 7.18, which nearly
649 agrees with Feng et al. [21] findings. The possession of free Ca^{2+} ions and their

650 concentration is related to the $\text{Ca}(\text{OH})_2$ dissolved and the alkalinity of the pore solution in
651 the matrix, which in turn produces more CaCO_3 which is considered the main dominant
652 healing product in samples.

653 The crack closure results revealed also unique trends based on Fig.8. Mixes BC,
654 PVAC2, and BC + PVAC1 showed the maximum crack closure and the disappearance of
655 crack propagation onto the surface of the cube specimens as shown in Fig. 8-a, b, and e.
656 Similarly, the mixes PVAC1 and PVAC1.5 showed the healing of some cracks but in lower
657 number and width than that of the other mixes. Cracks with a maximum width of 0.3 mm
658 are not visible for all the specimens. This suggests that the self-healing bacteria and PVA
659 fibers along with the addition of fly ash as mineral admixtures have deposited the chemical
660 reaction form of calcium bicarbonate causing physical and chemical reactions to bond and
661 seal the cracks. These results agree with the findings of Feng et al. [21] and Qiu et al. [22].
662 Their result confirms the coupling effect of using bacteria and PVA, in addition to their
663 benefit to the crack healing process. Hence, the closure of the crack width would in turn
664 reduce the porosities and regain the compressive strength of the concrete mixture.

665

666 4.4 Flexural strength

667 Similar to compressive strength and more crucial is flexural strength as most of the
668 concrete structure elements are subjected to bending moments which generate tension on
669 concrete causing cracking. Fig. 9 shows the results of the pre-damaged and undamaged
670 prism specimens for flexural at 7, 28, and 56 days of age. It should be mentioned that the
671 curing methods adopted as per the age of testing expect for 7 days the healing process took
672 around 28 days of age after pre-damaging the specimens.

673 Compared with the control mix, it is clear from Fig. 9-a, b, and c, that the undamaged
674 specimens attain a value of 73, 61, 54, 40, and 67% for mixes BC, PVAC1, PVAC1.5,
675 PVAC2, and BC+PVAC1 of that of the control mix at 7 days of age. Similarly, at 28 days
676 of age, the undamaged cube specimen for mixes BC, PVAC1, PVAC1.5, PVAC2, and
677 BC+PVAC1 revealed a value of 62, 64, 52, 54, and 63%, respectively. Finally, the
678 undamaged cube specimen at 56 days of age provided a value of 62, 55, 40, 33, and 59% of
679 that of control for mixes BC, PVAC1, PVAC1.5, PVAC2, and BC+PVAC1, respectively.

680 Feng et al. [21] explored the repaired area in prism specimens for those with bacteria
681 and PVA fibers and with coupled inclusion through a prism specimen tested in bending to
682 create mid-crack. The exploration was performed by stereo microscopic and binarization
683 images of crack surfaces to measure the crack width and the repaired area. In general, their
684 results revealed that the control specimens retained 31% on average of their crack repaired
685 after 7 and 28 days of age which was attributed to the continuous hydration of cement paste
686 carried out in the crack inner surfaces and carbonization reaction. However, the prism
687 specimens with PVA fibers achieved about 44 to 50 % at 7 and 28 days of age indicating
688 the improvement of the healing process using the PVA fibers. In the current study, the crack
689 width was measured as shown in Fig. 10. The crack width closure reached nearly 95% of

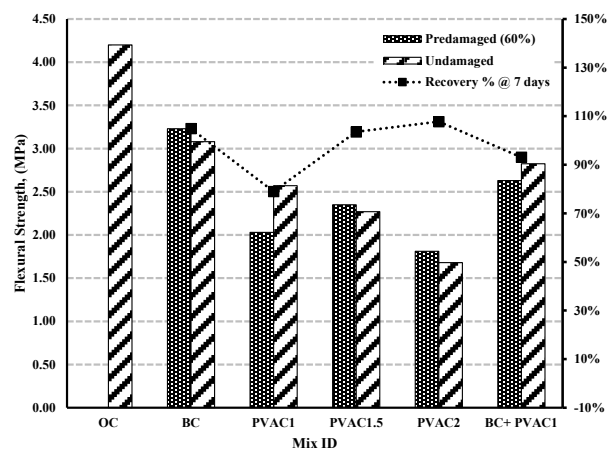
690 that of the original crack width. Similar findings were found in the literature [14, 22, 61]
691 that the PVA fibers provided the most reliable healing and recovery enhancement among
692 the other fibers (i.e., PP fiber, etc.). Feng et al. [21] also reported that the mixtures with
693 bacteria provided more repaired areas achieving over 50 and 74 % of the cracked area after
694 7 and 28 days of implementing the healing process. These findings were similar to those
695 observed by Luo et al. [61].

696 From Fig.9, the flexural strength of prism specimens for BC mix gains strength recovery
697 of 105, 124, and 124% after the healing at 7, 28, and 56 days of age. While those with added
698 PVA fiber at 1, 1.5, and 2% the recovery at 7 days were 79, 84, 97, 104, 85, 111, 108, 90,
699 and 148%, respectively for mix PVAC1, PVAC1.5, and PVAC2 at 7, 28 and 56 days of age.

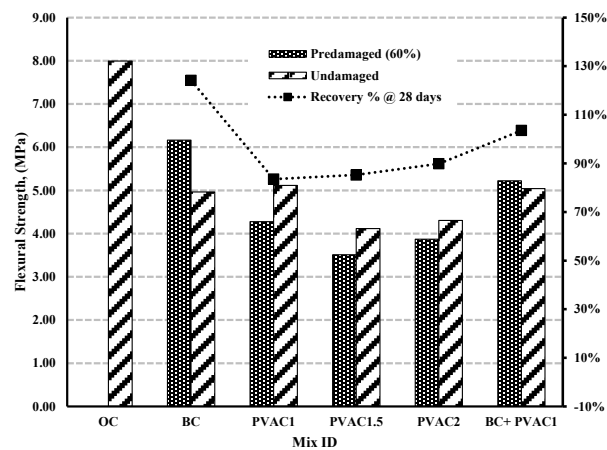
700 Feng et al. [21] also observed the coupling of the effect through the mortars with a
701 combination of PVA fiber and bacteria which attain a higher healing area of the cracks for
702 the prism specimens than those with PVA fibers only, reaching 55.2% and 64.6% at 7 and
703 28 days of age. Nevertheless, their observation showed lower values of repaired area for
704 cracks in prism specimens than those with bacteria only. Their reasons were around two
705 main aspects; one was that bacteria induced more calcium carbonate into those mixes with
706 fibers and the second was the fiber attracted some calcium ions dissolved and captured on
707 the fiber surface deposited within the inner crack surface which in turn inhibited the bacteria
708 activity and produced lower calcium carbonate concentration on the inner crack surface than
709 those mixes with bacteria only. This behaviour would be ascribed to the larger particle size
710 of calcium carbonate possess by the PVA fibers in addition to the absorption property which
711 the PVA fiber might utilize in absorbing more bacteria accelerating the precipitation of
712 carbon dioxide on the crack surface and initiating the generation of calcium carbonate.

713 The mechanism was discussed by several researchers [21, 62 – 64, 65]. For instance,
714 Feng et al. [21] studied the prism specimen under bending as stated earlier, and showed the
715 results provided un-damaged and cracked specimens. In general, all of the specimens with
716 bacteria, PVA fibers, or a combination of both showed lower flexural values than those of
717 the control which agrees with the current study. They attributed that the bacteria medium
718 would have encountered an adverse influence on the flexural capacity of the mixtures. This
719 behaviour was observed by the uneven distribution and volume expansion initiated by the
720 calcium carbonate inclusion resulting in microcracks in the carbonated zone [62 – 64].
721 Similarly, the PVA fiber mixture provided some voids due to the volume fraction, and thus,
722 the same observation was denoted for the mixture with both bacteria and PVA fiber in which
723 the flexural strength of the prism specimens is lower than that of the control. The behaviour
724 as clarified earlier is similar to the result attained in the current study; however, there was
725 no opportunity to measure the cracking area using stereo microscopic and binarization
726 images of crack surfaces. Nonetheless, the PVA fiber cracked/pre-damaged specimens
727 attain the role of stress transferring crossing the cracks in a bridging manner while
728 preventing crack propagation which influences the flexural strength capacity relevant to the

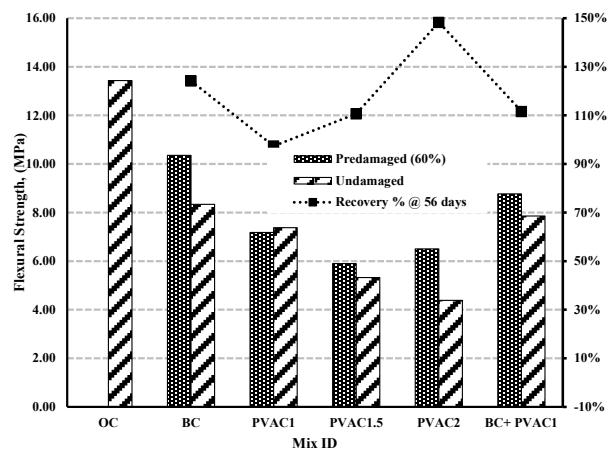
729 cracked/pre-damaged specimens with bacteria and combined; bacteria and PVA after
 730 implying wet/dry cycle regime [65].



(a) 7 days*



(b) 28 days



(c) 56 days

*The 7 days of age curing was then encountered in the healing process (dry and wet cycle) for 28 days

731 Fig. 9. Flexural strength results for the prism specimens for all mixes after hardening with
732 (pre-damaged) and without (undamaged) applying the healing process at (a) 7, (b) 28, and
733 (c) 56 days of age.

734 However, the mixes with bacteria and PVA fiber provided a lower flexural strength
735 compared to those of PVA fiber only. Flexural recovery attained by mixes with PVA1 fiber
736 and bacteria was 23%, which was slightly lower than that for specimens with PVA1 fiber
737 only (24%). Thus, it was concluded that fiber addition played a vital role in flexural
738 recovery, especially with crack widths reaching 0.4 ± 0.1 mm. Similar results were deduced
739 when investigating the coupling effect of bacteria and PVA fiber which proved an
740 insignificant influence on the flexural regain [66]. This was relevant to the surface
741 mineralization treatment with calcium carbonate [66] and the precipitation amount on PVA
742 fiber surfaces, concluding better performance to those of PVA fiber than those of bacteria
743 and PVA fiber combined. Further, Chen et al. [67] reported that immobilizing the bacteria
744 could retain 72% of the flexural recovery while 50 to 80% when adding fibers [68].

745 In conclusion, selecting the carrier for products possessed by bacteria would result in
746 enhancing the flexural regain of the cracked mixture, hence, the coupling influence of
747 bacteria and PVA fiber was observed in the high crack area closure rate.

748



749 Fig. 10. Crack closure of prism specimens at initiating cracks and after applying the
750 healing process at 28 days of age for mix BC + PVAC1

751 The mix BC + PVAC1 was recovered by 93, 104, and 112% at 7, 28, and 56 days of
752 age. Thus, the BC + PVAC1 provided the highest compressive strength recovery. It should
753 be mentioned that the OC mix might have provided a greater grade at failure stress than
754 other mixes with BC and PVA addition at 7 days of age. Due to the difficulty in measuring
755 and getting more photos for the flexural prism specimens before and after the healing
756 process, only mix BC+PVAC is presented, as shown in Fig.10. The figure shows the closure
757 of the crack of 0.3865 mm after 28 days of curing exposed to wet and dry cycle have reached
758 to 0.0714 which means that nearly 95% of the crack width was closed and filled with PVA
759 and the bacterial reaction that possessed more calcites as illustrated by Zhang et al. [59].

760 It should be noted that Shaaban et al. [69] revealed similar results in terms of
761 compressive and flexural strength for the bacterial mix; Mix BC as their results provided a

762 high gain in strengths when using *B. subtilis* at 10^8 cells/ml, not 10^5 cells/ml as per their
763 investigation and experimental program which is similar to the findings in both compressive
764 and flexural strengths revealed here in this study.

765 4.5 Absorption Percentile

766 Absorption is one term that can determine and evaluate the durability of concrete. An
767 average of three cube specimens was reported. The test surfaces should be at the same
768 distance as the exposed distance from the original exposed surface of the concrete. Then,
769 the specimens should be handled in an environmental chamber at a temperature of 50°C and
770 relative humidity of 80% for three days and then sealed in that specimen. The specimens
771 are arranged with a space to allow for airflow in between and stored at room temperature.

772

773

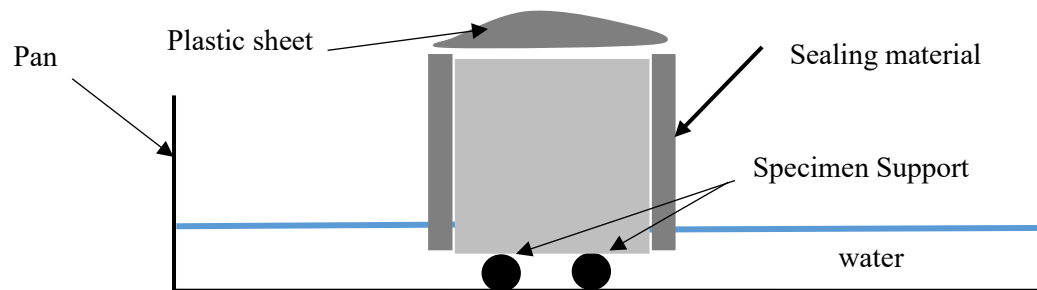
774

775

776

777

778



779

Fig. 11. A typical cube specimen under absorption testing

780

781

782

783

784

785

786

After a minimum of 15 days, the specimens were vacuumed while sealing the end face with plastic sheets using a vacuum pump for 3 hours and exposing it to tap water through the vacuum chamber. The specimens were soaked for 18 hours underwater and then weighed the specimen. The side surface and one end that is not exposed to water were sealed with a plastic sheet that can be secured using an elastic band. The initial mass was weighed and then specimens were placed into tap water with a height of 3 mm using supports. Then the specimens were weighted at several intervals of time [41], as shown in Fig. 11.

787

788

789

790

791

792

793

794

795

796

797

798

799

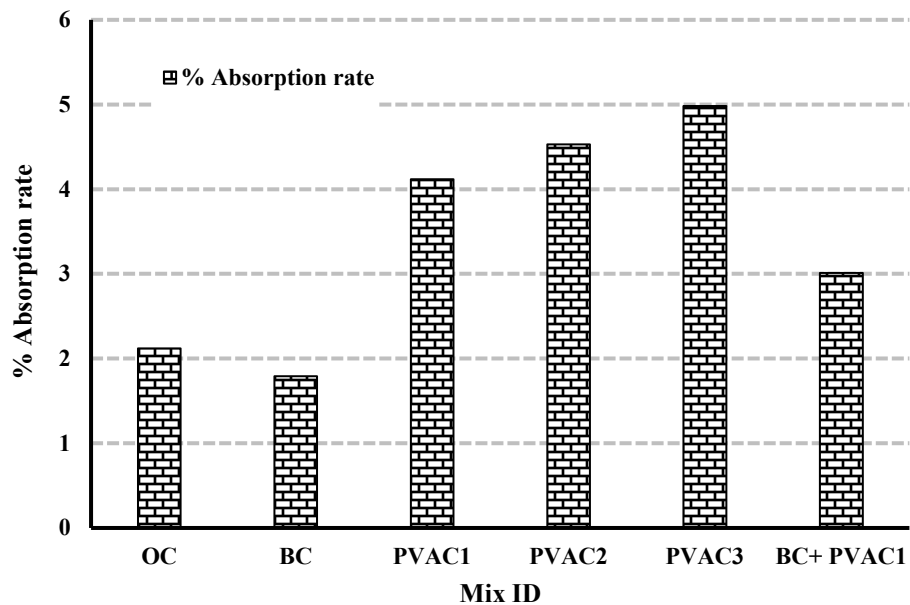
800

801

802

The records are then plotted and presented, as shown in Fig. 12. Absorption rate for the bacterial mix showed the lowest values among all the mixes which means that the bacteria possessed a reaction that would increase the existence of more calcite closing all the pores inside the concrete or at least the network between pores would be closed. On the other hand, the mixes PVAC1, PVAC1.5, and PVAC2 which contain PVA fibers would have a higher absorption rate than the other mixes including the control "OC". This is attributed to the absorption rate of the fiber itself stated by Jain et al.[70], Shen et al.[71], and Li et al.[72]. They stated that the PVA fibers have a high intake of water and can reach 41.97 % moisture adsorption content at 8 hours of water exposure. They confirmed that the outer pure PVA tissue would get saturated for longer water exposure of water. Nevertheless, adding the bacteria with the lowest percentile of PVA (1%) as in mixBC+PVAC1 the absorption rate would be reduced reaching a minimized value between those of mixes BC and PVAC1. It should be mentioned that mix PVAC1 showed the lowest among the mixes with PVA fibers as it contains the lowest volume fraction of 1% while the other contains 1.5% and 2%. From the results, it is very clear the effectiveness of using PVA fibers in healing the concrete.

803 On the other hand, Feng et al. [21] have measured both the absorption and sorptivity of
 804 the mixes. Their results revealed that the absorption with the control specimen was the
 805 highest among all the other mixes and the absorption rate reduced with time. Similarly the
 806 specimens for mix with bacteria but still lower compared to the control specimens. They
 807 attributed this reduction to the fact that the precipitated calcium carbonate is conducive to
 808 reducing water uptake on the surfaces and inner cracks induced by bacteria, in addition to,
 809 the swelling due to pore size reduction [73, 74]. The absorption for mixes with PVA fiber
 810 was lower than that of control since fiber could refine the pore structure by subdividing
 811 them into small pores [75], in contrast to the current results here in this study, in which the
 812 PVA fiber showed higher absorption due to the absorption property attained by the PVA
 813 fiber. Feng et al. [21] results confirmed that the fiber diameter influenced the absorption
 814 reduction the lower the diameter the higher the absorption reduction. This action was
 815 demonstrated by well-dispersed shorter fiber that could increase the tortuosity and
 816 roughness of cracks. This behaviour would in turn reduce the rate of water surpassing the
 817 cracks [76, 77]. Their results, also, revealed that the fiber provided more efficiency in
 818 improving the water tightness of cracked mortars than those of mixes with bacteria since
 819 the absorption rate of mixes with fiber showed lower values than those of bacteria. On the
 820 other hand, the mixes in which both bacteria and fiber provided lower absorption than those
 821 mixes with fiber or bacteria only. In conclusion, their investigation reported that the
 822 inclusion of both PVA fiber and bacteria efficiently enhanced the water tightness for healed
 823 cracks by sealing the voids and pores.



824

825

Fig. 12. Absorption rate of the mixes at 28 days

826 **4.6 Sorptivity**

827

828

829

830

Sorptivity, or capillary suction, is the transport of liquids in porous solids due to surface tension acting in capillaries [78]. It is a function of the viscosity, density, and surface tension of the liquid, and the pore structure (radius, tortuosity, and continuity of capillaries) of the solid [78]. Sorptivity is a material's ability to absorb and transmit water through it via

831 capillary suction and provides an engineering measure of microstructure and properties
832 important for durability[79]. Sorptivity is increasingly being used as a measure of concrete
833 resistance to exposure to aggressive environments. The water sorptivity test is a
834 unidirectional absorption test [79, 80]. Usually, the specimens are coated with epoxy from
835 their sides and placed into water and Ca (OH)₂ to measure the suction rate of water using
836 capillary conceptual. Fig. 13 shows the specimen under testing while pressuring the water
837 for testing sorptivity and evaluation rate of absorption unidirectional using scaled grade as
838 per ASTM C1585 [80] regulations.

839



840 Fig. 13. A typical cube specimen under sorptivity testing [79, 80]

841

842 Fig. 14 shows the depth value exposed to water because of suction capillary action for
843 the cube specimen of each mix among the six mixes. The mixes showed a similar results
844 trend to the absorption rate. The mix BC showed a lower suction rate as the pores mostly
845 was closed by calcites [70]. The mixes with PVA fiber showed high suction rates especially
846 those with high VF (2%) as in mix PVAC2. The addition of BC to the PVA fiber as in the
847 mix BC+PVAC1 provided a suction rate nearly to that of mix BC which means that the
848 bacteria have a high influence in reducing the absorption rate of the PVA fiber because of
849 depositing more calcite onto the surface of PVA fibers [38].

850 Few researchers have studied the sorptivity [21, 22, 81, 82]. Feng et al. [21] explored
851 the sorptivity of the cracked specimens after healing for 28 days and found similar trends to
852 those of absorption results. On the other hand, un-damaged specimens for mixes with
853 bacteria showed a higher rate of sorptivity than that of control samples. In other words, the
854 bacteria inclusion provides lower water resistance than the control specimens since
855 retarding effect occurred by sucrose [81, 82] in the bacterial medium.

856 However, mixes with bacteria or PVA fiber or both provided conversely, lower rates
857 than that of control samples at reduction values below 50%, in contrast to 120% for the
858 control specimens which means a significant increase in initial sorptivity coefficient for
859 samples after cracking. Specimens with PVA1 fiber and bacteria showed lower sorptivity
860 coefficient values than those of samples with PVA1 fiber or bacteria respectively. It
861 indicated that the coupling effect of bacteria and PVA1 fiber could be conducive to an
862 increased water resistance of mortars. Comparing results of area repair rate, capillary water
863 absorption, and sorptivity reduction for self-healing, it could be inferred that more calcium
864 carbonate precipitated in the inner instead of surfaces of cracks for specimens with fiber and
865 bacteria compared to those specimens with bacteria only.

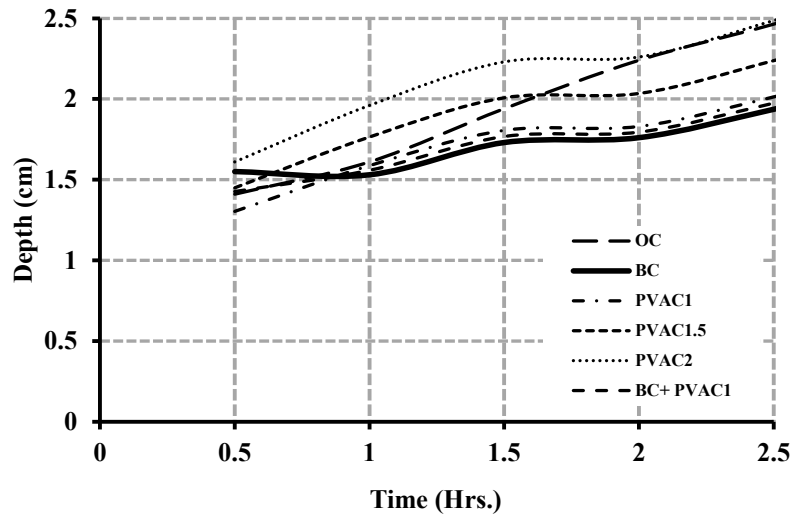


Fig. 14 Depth exposed to water

866

867

868 5. Conclusion and key findings

869 The study consisted of six mixes that were cast, including control mix, *B. subtilis*
 870 bacteria, and PVA fiber addition at various percentile (1, 1.5, and 2%). The sixth mix
 871 presented the coupling effect where the bacteria and the mixes with PVA fiber addition at
 872 VF of 1% were combined. Mechanical properties in terms of compressive and flexural
 873 strengths at 7, 28, and 56 days were evaluated after initiating cracks and the healing process
 874 applied. Furthermore, durability testing was carried out through absorption rate and
 875 sorptivity evaluation for the specimens after exposure to the healing process of wet and dry
 876 cycle curing at 28 days. The results provided in terms of mechanical properties and
 877 durability of concrete revealed that the coupling would provide optimized results between
 878 those using bacteria and PVA fiber addition. Nevertheless, bacteria production requires a
 879 very difficult process for cultivation and growth as well as serious precautions such as the
 880 environment of adding the bacteria in concrete would be damaged while mixing. However,
 881 the results showed the following:

882 In terms of fresh state properties, the addition of bacteria and PVA fibers reduced the
 883 workability, and it was recommended to use the superplasticizer in this case. Yet no
 884 researcher investigated the different types of waster-reducer based on the bacteria
 885 environment or their influence on the PVA fiber addition while being added with fly ash as
 886 a mineral admixture.

887 It was observed that the density revealed nearly similar values to that of the control;
 888 however, when adding the PVA fibers the density decreases due to the PVA fiber specific
 889 gravity and the lower density is due to the creation of more voids when using the PVA
 890 fibers.

891 The mechanical properties of both the comprehensive and flexural strength revealed a
 892 similar trend. The results revealed that the coupled effect would provide an optimized
 893 strength in between the PVA of 1% and Bacteria with a count of 1.08×10^8 cells/ml, solution
 894 concentration of 600 nm/liter. The best performance was revealed with those of bacteria
 895 addition and resulted in enhanced strength compared with that obtained with the other

896 mixes; however, precautions should be taken during production. The second mix is one with
897 a PVA addition of 2%; however, ball formation might be the reason for the reduction of its
898 general grading from the very beginning as noticed when compared to the strength of
899 conventional concrete. Nevertheless, it provides increased strength with age (56 days).

900 The durability evaluation of concrete in terms of sorptivity and absorption rate indicated
901 the influence of the bacteria was better than that of PVA fiber addition. The durable concrete
902 should have lower sorptivity and low rate of absorption; however, due to the PVA fiber
903 behaviour for the intake of water, both the sorptivity and the absorption rate were affected.
904 The addition of bacteria, on the other hand, lowered the sorptivity instead along the cycle
905 period.

906 Further investigation is required to study the techniques on an individual and coupled
907 basis for further implementation of techniques in repairing the deteriorated concrete
908 structures and how it would deal with the corroded steel reinforcement on short and long-
909 term behaviour

910 **In summary, the key findings from the investigation are as follows:**

911 The bacterial self-healing mechanism facilitates pore closure in the concrete matrix by
912 precipitating calcite crystals that grow and spread from nucleation sites on the bacterial cell
913 walls.

914 This crystallization process progressively seals pores and cracks, reducing pathways for
915 moisture ingress.

916 The coupling effect, consisting of combining the bacteria and the mixes with PVA fiber
917 addition at VF of 1%, provides optimized results between those using bacteria and PVA
918 fiber addition.

919 In terms of fresh state properties, the addition of bacteria and PVA fibers reduced the
920 workability, and it was recommended to use the superplasticizer in this case.

921 With regards to the durability of the concrete in terms of sorptivity and absorption rate,
922 the addition of bacteria has a more positive impact than that of the PVA fibers.

923 **Compliance with Ethical Standards**

- 924 - The authors declare that they have no conflict of interest.
- 925 - This article does not contain any studies with human participants or animals performed
926 by any of the authors.
- 927 - The authors declare that they have no known competing financial interests or personal
928 relationships that could have appeared to influence the work reported in this paper.

929 **References**

930 [1] Mihashi, H., & Nishiwaki, T. (2012). Development of Engineered Self-Healing and Self-
931 Repairing Concrete-State-of-the-Art Report. In Journal of Advanced Concrete
932 Technology (Vol. 10, Issue 5, pp. 170–184). Japan Concrete Institute.
933 <https://doi.org/10.3151/jact.10.170>

934 [2] Nishiwaki, T., Kwon, S., Homma, D., Yamada, M., & Mihashi, H. (2014). Self-Healing
935 Capability of Fiber-Reinforced Cementitious Composites for Recovery of Watertightness

- 936 and Mechanical Properties. In *Materials* (Vol. 7, Issue 3, pp. 2141–2154). MDPI AG.
937 <https://doi.org/10.3390/ma7032141>
- 938 [3] Van Tittelboom, K., & De Belie, N. (2013). Self-Healing in Cementitious Materials—A
939 Review. In *Materials* (Vol. 6, Issue 6, pp. 2182–2217). MDPI AG.
940 <https://doi.org/10.3390/ma6062182>
- 941 [4] Roig-Flores, M., Formagini, S., & Serna, P. (2021). Self-healing concrete-What Is it Good
942 For? In *Materiales de Construcción* (Vol. 71, Issue 341, p. e237). Editorial CSIC.
943 <https://doi.org/10.3989/mc.2021.07320>
- 944 [5] C. Edvardsen, “Water Permeability and Autogenous Healing of Cracks in Concrete.
945 (1999). In *ACI Materials Journal* (Vol. 96, Issue 4). American Concrete Institute.
946 <https://doi.org/10.14359/645>
- 947 [6] De Belie, N., Gruyaert, E., Al-Tabbaa, A., Antonaci, P., Baera, C., Bajare, D., Darquennes,
948 A., Davies, R., Ferrara, L., Jefferson, T., Litina, C., Miljevic, B., Otlewska, A., Ranogajec,
949 J., Roig-Flores, M., Paine, K., Lukowski, P., Serna, P., Tulliani, J., ... Jonkers, H. M.
950 (2018). A Review of Self-Healing Concrete for Damage Management of Structures. In
951 *Advanced Materials Interfaces* (Vol. 5, Issue 17). Wiley.
952 <https://doi.org/10.1002/admi.201800074>
- 953 [7] Wiktor, V., & Jonkers, H. M. (2011). Quantification of crack-healing in novel bacteria-
954 based self-healing concrete. In *Cement and Concrete Composites* (Vol. 33, Issue 7, pp.
955 763–770). Elsevier BV. <https://doi.org/10.1016/j.cemconcomp.2011.03.012>
- 956 [8] Nishiwaki, T., Mihashi, H., Jang, B.-K., & Miura, K. (2006). Development of a Self-
957 Healing System for Concrete with Selective Heating around Crack. In *Journal of*
958 *Advanced Concrete Technology* (Vol. 4, Issue 2, pp. 267–275). Japan Concrete Institute.
959 <https://doi.org/10.3151/jact.4.267>
- 960 [9] Nishiwaki, T., Mihashi, H., & Okuhara, Y. (2010). Fundamental study on self-repairing
961 concrete using a selective heating device. In *Concrete Under Severe Conditions, Two*
962 *Volume Set* (pp. 919–926). CRC Press. <https://doi.org/10.1201/b10552-116>
- 963 [10] Dry, C. M. (2000). Three designs for the internal release of sealants, adhesives, and
964 waterproofing chemicals into concrete to reduce permeability. In *Cement and Concrete*
965 *Research* (Vol. 30, Issue 12, pp. 1969–1977). Elsevier BV. [https://doi.org/10.1016/s0008-](https://doi.org/10.1016/s0008-8846(00)00415-4)
966 [8846\(00\)00415-4](https://doi.org/10.1016/s0008-8846(00)00415-4)
- 967 [11] Van Tittelboom, K., De Belie, N., Van Loo, D., & Jacobs, P. (2011). Self-healing
968 efficiency of cementitious materials containing tubular capsules filled with healing agent.
969 In *Cement and Concrete Composites* (Vol. 33, Issue 4, pp. 497–505). Elsevier BV.
970 <https://doi.org/10.1016/j.cemconcomp.2011.01.004>
- 971 [12] Joseph, C., Jefferson, A. D., Isaacs, B., Lark, R., & Gardner, D. (2010). Experimental
972 investigation of adhesive-based self-healing of cementitious materials. In *Magazine of*
973 *Concrete Research* (Vol. 62, Issue 11, pp. 831–843). Thomas Telford Ltd.
974 <https://doi.org/10.1680/mac.2010.62.11.831>
- 975 [13] Homma, D., Mihashi, H., & Nishiwaki, T. (2009). Self-Healing Capability of Fibre
976 Reinforced Cementitious Composites. In *Journal of Advanced Concrete Technology*
977 (Vol. 7, Issue 2, pp. 217–228). Japan Concrete Institute. <https://doi.org/10.3151/jact.7.217>

- 978 [14] Nishiwaki, T., Koda, M., Yamada, M., Mihashi, H., & Kikuta, T. (2012). c on Self-
979 Healing Capability of FRCC Using Different Types of Synthetic Fibers. In *Journal of*
980 *Advanced Concrete Technology* (Vol. 10, Issue 6, pp. 195–206). Japan Concrete Institute.
981 <https://doi.org/10.3151/jact.10.195>
- 982 [15] Mauser, T., Déjugnat, C., & Sukhorukov, G. B. (2004). Reversible pH-Dependent
983 Properties of Multilayer Microcapsules Made of Weak Polyelectrolytes. In
984 *Macromolecular Rapid Communications* (Vol. 25, Issue 20, pp. 1781–1785). Wiley.
985 <https://doi.org/10.1002/marc.200400331>
- 986 [16] Liang, K., Such, G. K., Johnston, A. P. R., Zhu, Z., Ejima, H., Richardson, J. J., Cui, J.,
987 & Caruso, F. (2013). Endocytic pH-Triggered Degradation of Nanoengineered Multilayer
988 Capsules. In *Advanced Materials* (Vol. 26, Issue 12, pp. 1901–1905). Wiley.
989 <https://doi.org/10.1002/adma.201305144>
- 990 [17] Hammad, N., Elnemr, A., & Shaaban, I. G. (2023). State-of-the-Art Report: The Self-
991 Healing Capability of Alkali-Activated Slag (AAS) Concrete. In *Materials* (Vol. 16, Issue
992 12, p. 4394). MDPI AG. <https://doi.org/10.3390/ma16124394>
- 993 [18] Dong, B., Wang, Y., Fang, G., Han, N., Xing, F., & Lu, Y. (2015). Smart releasing
994 behaviour of a chemical self-healing microcapsule in the stimulated concrete pore
995 solution. In *Cement and Concrete Composites* (Vol. 56, pp. 46–50). Elsevier BV.
996 <https://doi.org/10.1016/j.cemconcomp.2014.10.006>
- 997 [19] Lv, L., Yang, Z., Chen, G., Zhu, G., Han, N., Schlangen, E., & Xing, F. (2016). Synthesis
998 and characterization of a new polymeric microcapsule and feasibility investigation in self-
999 healing cementitious materials. In *Construction and Building Materials* (Vol. 105, pp.
1000 487–495). Elsevier BV. <https://doi.org/10.1016/j.conbuildmat.2015.12.185>
- 1001 [20] Xu, N., Song, Z., Guo, M.-Z., Jiang, L., Chu, H., Pei, C., Yu, P., Liu, Q., & Li, Z. (2021).
1002 Employing ultrasonic wave as a novel trigger of microcapsule self-healing cementitious
1003 materials. In *Cement and Concrete Composites* (Vol. 118, p. 103951). Elsevier BV.
1004 <https://doi.org/10.1016/j.cemconcomp.2021.103951>
- 1005 [21] Feng, J., Su, Y., & Qian, C. (2019). Coupled effect of PP fiber, PVA fiber and bacteria
1006 on self-healing efficiency of early-age cracks in concrete. In *Construction and Building*
1007 *Materials* (Vol. 228, p. 116810). Elsevier BV.
1008 <https://doi.org/10.1016/j.conbuildmat.2019.116810>
- 1009 [22] Qiu, J., Tan, H. S., & Yang, E.-H. (2016). Coupled effects of crack width, slag content,
1010 and conditioning alkalinity on autogenous healing of engineered cementitious
1011 composites. In *Cement and Concrete Composites* (Vol. 73, pp. 203–212). Elsevier BV.
1012 <https://doi.org/10.1016/j.cemconcomp.2016.07.013>
- 1013 [23] BS-EN197-1, (2011) “Cement Part 1: Composition, Specifications and Conformity
1014 Criteria for Common Cements,” Br. Stand., no. November, 2011.
- 1015 [24] Egyptian Standards ES 4756-1/2007, Cement Part 1: Composition, Specifications and
1016 Conformity Criteria for common cements. Egyptian Organization for Standards &
1017 Quality, Arab Republic of Egypt, 2007.
- 1018 [25] ASTM C168, (2022). Terminology Relating to Thermal Insulation. ASTM International.
1019 <https://doi.org/10.1520/c0168-22>

- 1020 [26] ASTM C33, (2018). Specification for Concrete Aggregates. ASTM International.
1021 https://doi.org/10.1520/c0033_c0033m-18.
- 1022 [27] BS EN 933-1, (2012) "Tests for geometrical properties of aggregates Determination of
1023 particle size distribution. Sieving method", Br. Stand., 2012
- 1024 [28] ASTM C117, (2017). Test Method for Materials Finer than 75- μ m (No. 200) Sieve in
1025 Mineral Aggregates by Washing. ASTM International. <https://doi.org/10.1520/c0117-17>.
- 1026 [29] ASTM C127, (2015). Test Method for Relative Density (Specific Gravity) and
1027 Absorption of Coarse Aggregate. ASTM International. <https://doi.org/10.1520/c0127-15>
- 1028 [30] ASTM C128, (2022). Test Method for Relative Density (Specific Gravity) and
1029 Absorption of Fine Aggregate. ASTM International. <https://doi.org/10.1520/c0128-22>.
- 1030 [31] BS 812-2, (1999) British Standards Institution BSI, "BS 812: Part 2:1995 Testing
1031 aggregates, Methods of determination of density," Br. Stand., no. 105, 1999.
- 1032 [32] BS 812-103, (1989) "Testing aggregates — Part 103: Method for determination of
1033 particle size distribution — Section 103.2 Sedimentation test," Br. Stand., no. 1, 1989.
- 1034 [33] Tian, H., Zhang, Y. X., Ye, L., & Yang, C. (2015). Mechanical behaviours of green hybrid
1035 fibre-reinforced cementitious composites. In *Construction and Building Materials* (Vol.
1036 95, pp. 152–163). Elsevier BV. <https://doi.org/10.1016/j.conbuildmat.2015.07.143>.
- 1037 [34] Chen, Y., & Qiao, P. (2011). Crack Growth Resistance of Hybrid Fiber-Reinforced
1038 Cement Matrix Composites. In *Journal of Aerospace Engineering* (Vol. 24, Issue 2, pp.
1039 154–161). American Society of Civil Engineers (ASCE).
1040 [https://doi.org/10.1061/\(asce\)as.1943-5525.0000031](https://doi.org/10.1061/(asce)as.1943-5525.0000031)
- 1041 [35] Khan, M., Cao, M., & Ali, M. (2020). Cracking behaviour and constitutive modelling of
1042 hybrid fibre reinforced concrete. In *Journal of Building Engineering* (Vol. 30, p. 101272).
1043 Elsevier BV. <https://doi.org/10.1016/j.jobe.2020.101272>
- 1044 [36] ACI 211.1-91, "Standard Practice for Selecting Proportions for Normal Heavyweight,
1045 and Mass Concrete (ACI 211.1-91) Reapproved 1997," ACI Comm. Rep., 1997.
- 1046 [37] Srinivasa, C. H., & Venkatesh. (2022). Prediction of Compressive Strength of Polyvinyl
1047 Alcohol Fiber Reinforced Bendable Concrete. In *IOP Conference Series: Earth and
1048 Environmental Science* (Vol. 982, Issue 1, p. 012007). IOP Publishing.
1049 <https://doi.org/10.1088/1755-1315/982/1/012007>
- 1050 [38] Zhou, S., Zhu, H., Ju, J. W., Yan, Z., & Chen, Q. (2017). Modeling microcapsule-enabled
1051 self-healing cementitious composite materials using discrete element method. In
1052 *International Journal of Damage Mechanics* (Vol. 26, Issue 2, pp. 340–357). SAGE
1053 Publications. <https://doi.org/10.1177/1056789516688835>
- 1054 [39] British Standards Institution BSI, "Testing hardened concrete - Part 2: Making and curing
1055 specimens for strength tests," BS En 12390-2 2009, 2009.
- 1056 [40] ASTM C143/C143M, (2012). Test Method for Slump of Hydraulic-Cement Concrete.
1057 ASTM International. https://doi.org/10.1520/c0143_c0143m-12
- 1058 [41] ASTM C642, (2021). Test Method for Density, Absorption, and Voids in Hardened
1059 Concrete. ASTM International. <https://doi.org/10.1520/c0642-21>

- 1060 [42] Kim, D. J., Park, S. H., Ryu, G. S., & Koh, K. T. (2011). Comparative flexural behaviour
1061 of Hybrid Ultra High Performance Fiber Reinforced Concrete with different macro fibers.
1062 In *Construction and Building Materials* (Vol. 25, Issue 11, pp. 4144–4155). Elsevier BV.
1063 <https://doi.org/10.1016/j.conbuildmat.2011.04.051>
- 1064 [43] Sharaky, I. A., Ahmad, S. S., El-Azab, A. M., & Khalil, H. S. (2021). Strength and Mass
1065 Loss Evaluation of HSC with Silica Fume and Nano-Silica Exposed to Elevated
1066 Temperatures. In *Arabian Journal for Science and Engineering* (Vol. 47, Issue 4, pp.
1067 4187–4209). Springer Science and Business Media LLC. [https://doi.org/10.1007/s13369-
1068 021-06006-7](https://doi.org/10.1007/s13369-021-06006-7).
- 1069 [44] Pakravan, H. R., Latifi, M., & Jamshidi, M. (2014). Ductility improvement of
1070 cementitious composites reinforced with polyvinyl alcohol-polypropylene hybrid fibers.
1071 In *Journal of Industrial Textiles* (Vol. 45, Issue 5, pp. 637–651). SAGE Publications.
1072 <https://doi.org/10.1177/1528083714534712>.
- 1073 [45] BS EN 12390-2019 Part 3, “Testing hardened concrete: Compressive strength of test
1074 specimens,” Br. Stand. Inst., 2019.
- 1075 [46] ASTM C 78, (2009). Test Method for Flexural Strength of Concrete (Using Simple Beam
1076 with Third-Point Loading). ASTM International. <https://doi.org/10.1520/c0078-09>.
- 1077 [47] Liu, H.-K., Liao, W.-C., Tseng, L., Lee, W.-H., & Sawada, Y. (2004). Compression
1078 strength of pre-damaged concrete cylinders reinforced by non-adhesive filament wound
1079 composites. In *Composites Part A: Applied Science and Manufacturing* (Vol. 35, Issue 2,
1080 pp. 281–292). Elsevier BV. [https://doi.org/10.1016/s1359-835x\(03\)00250-1](https://doi.org/10.1016/s1359-835x(03)00250-1)
- 1081 [48] Ma, G., Li, H., Yan, L., & Huang, L. (2018). Testing and analysis of basalt FRP-confined
1082 damaged concrete cylinders under axial compression loading. In *Construction and
1083 Building Materials* (Vol. 169, pp. 762–774). Elsevier BV.
1084 <https://doi.org/10.1016/j.conbuildmat.2018.02.172>
- 1085 [49] Mesbah, H.-A., & Benzaid, R. (2017). Damage-based stress-strain model of RC cylinders
1086 wrapped with CFRP composites. *Advances in Concrete Construction*, 5(5), 539–561.
1087 <https://doi.org/10.12989/ACC.2017.5.5.539>
- 1088 [50] Yang, Y., Lepech, M. D., Yang, E.-H., & Li, V. C. (2009). Autogenous healing of
1089 engineered cementitious composites under wet–dry cycles. In *Cement and Concrete
1090 Research* (Vol. 39, Issue 5, pp. 382–390). Elsevier BV.
1091 <https://doi.org/10.1016/j.cemconres.2009.01.013>
- 1092 [51] Topič, J., Prošek, Z., Indrova, K., Plachý, T., Nežerka, V., Kopecký, L., & Tesárek, P.
1093 (2015). EFFECT OF PVA MODIFICATION ON PROPERTIES OF CEMENT
1094 COMPOSITES. In *Acta Polytechnica* (Vol. 55, Issue 1, pp. 64–75). Czech Technical
1095 University in Prague - Central Library. <https://doi.org/10.14311/ap.2015.55.0064>
- 1096 [52] Hussein, Z. M., Abedali, A. H., & Ahmead, A. S. (2019). Improvement Properties of Self
1097 -Healing Concrete by Using Bacteria. In *IOP Conference Series: Materials Science and
1098 Engineering* (Vol. 584, Issue 1, p. 012034). IOP Publishing.
1099 <https://doi.org/10.1088/1757-899x/584/1/012034>
- 1100 [53] Zhang, P., Li, Q., Wang, J., Shi, Y., & Ling, Y. (2019). Effect of PVA fiber on durability
1101 of cementitious composite containing nano-SiO₂. In *Nanotechnology Reviews* (Vol. 8,

- 1102 Issue 1, pp. 116–127). Walter de Gruyter GmbH. [https://doi.org/10.1515/ntrev-2019-](https://doi.org/10.1515/ntrev-2019-0011)
1103 [0011](https://doi.org/10.1515/ntrev-2019-0011)
- 1104 [54] Safiuddin, M., Ihteshaam, S., Kareem, R. A., & Shalam. (2022). A study on self-healing
1105 concrete. In *Materials Today: Proceedings* (Vol. 52, pp. 1175–1181). Elsevier BV.
1106 <https://doi.org/10.1016/j.matpr.2021.11.023>
- 1107 [55] Flatt R, Houst Y, Bowen P and HofmannH2000 Electrostatic repulsion induced by
1108 superplasticizers between cement particles – an overlooked mechanism?
1109 Sixth CANMET/ACI Int. Conf. on Superplasticizers and Other Chemical Admixtures in
1110 Concrete 195, 29–42
- 1111 [56] Neville, A.M. and Brooks, J.J. (2010) *Concrete Technology*. 2nd Edition, Pearson
1112 Education Ltd., London.
- 1113 [57] Yew, M. K., Bin Mahmud, H., Ang, B. C., & Yew, M. C. (2015). Effects of Low Volume
1114 Fraction of Polyvinyl Alcohol Fibers on the Mechanical Properties of Oil Palm Shell
1115 Lightweight Concrete. In *Advances in Materials Science and Engineering* (Vol. 2015, pp.
1116 1–11). Hindawi Limited. <https://doi.org/10.1155/2015/425236>
- 1117 [58] Shafiqh, P., Mahmud, H., & Jumaat, M. Z. (2011). Effect of steel fiber on the mechanical
1118 properties of oil palm shell lightweight concrete. In *Materials & Design* (Vol. 32,
1119 Issue 7, pp. 3926–3932). Elsevier BV. <https://doi.org/10.1016/j.matdes.2011.02.055>
- 1120 [59] Zhang, C., Liu, R., Chen, M., Li, X., & Zhu, Z. (2022). Coupled effect of self-healing
1121 granules and permeable crystalline additive on early-age cracks repair in cement material.
1122 In *Materials Letters* (Vol. 323, p. 132560). Elsevier BV.
1123 <https://doi.org/10.1016/j.matlet.2022.132560>
- 1124 [60] Bhaskar, S., Anwar Hossain, K. M., Lachemi, M., Wolfaardt, G., & Otini Kroukamp, M.
1125 (2017). Effect of self-healing on strength and durability of zeolite-immobilized bacterial
1126 cementitious mortar composites. In *Cement and Concrete Composites* (Vol. 82, pp. 23–
1127 33). Elsevier BV. <https://doi.org/10.1016/j.cemconcomp.2017.05.013>.
- 1128 [61] Luo, M., Qian, C., & Li, R. (2015). Factors affecting crack repairing capacity of bacteria-
1129 based self-healing concrete. In *Construction and Building Materials* (Vol. 87, pp. 1–7).
1130 Elsevier BV. <https://doi.org/10.1016/j.conbuildmat.2015.03.117>.
- 1131 [62] Fabbri, A., Corvisier, J., Schubnel, A., Brunet, F., Goffé, B., Rimmelé, G., & Barlet-
1132 Gouédard, V. (2009). Effect of carbonation on the hydro-mechanical properties of
1133 Portland cements. In *Cement and Concrete Research* (Vol. 39, Issue 12, pp. 1156–1163).
1134 Elsevier BV. <https://doi.org/10.1016/j.cemconres.2009.07.028>
- 1135 [63] Pei, R., Liu, J., Wang, S., & Yang, M. (2013). Use of bacterial cell walls to improve the
1136 mechanical performance of concrete. In *Cement and Concrete Composites* (Vol. 39, pp.
1137 122–130). Elsevier BV. <https://doi.org/10.1016/j.cemconcomp.2013.03.024>
- 1138 [64] Johannesson, B., & Utgenannt, P. (2001). Microstructural changes caused by carbonation
1139 of cement mortar. In *Cement and Concrete Research* (Vol. 31, Issue 6, pp. 925–931).
1140 Elsevier BV. [https://doi.org/10.1016/s0008-8846\(01\)00498-7](https://doi.org/10.1016/s0008-8846(01)00498-7)
- 1141 [65] Kakooei, S., Akil, H. M., Jamshidi, M., & Rouhi, J. (2012). The effects of polypropylene
1142 fibers on the properties of reinforced concrete structures. In *Construction and Building*

- 1143 Materials (Vol. 27, Issue 1, pp. 73–77). Elsevier BV.
1144 <https://doi.org/10.1016/j.conbuildmat.2011.08.015>
- 1145 [66] Sambudi, N. S., Park, S. B., & Cho, K. (2016). Enhancing the mechanical properties of
1146 electrospun chitosan/poly(vinyl alcohol) fibers by mineralization with calcium carbonate.
1147 In *Journal of Materials Science* (Vol. 51, Issue 16, pp. 7742–7753). Springer Science and
1148 Business Media LLC. <https://doi.org/10.1007/s10853-016-0056-8>.
- 1149 [67] Chen, H., Qian, C., & Huang, H. (2016). Self-healing cementitious materials based on
1150 bacteria and nutrients immobilized respectively. In *Construction and Building Materials*
1151 (Vol. 126, pp. 297–303). Elsevier BV.
1152 <https://doi.org/10.1016/j.conbuildmat.2016.09.023>.
- 1153 [68] Wang, J., Van Tittelboom, K., De Belie, N., & Verstraete, W. (2012). Use of silica gel or
1154 polyurethane immobilized bacteria for self-healing concrete. In *Construction and*
1155 *Building Materials* (Vol. 26, Issue 1, pp. 532–540). Elsevier BV.
1156 <https://doi.org/10.1016/j.conbuildmat.2011.06.054>
- 1157 [69] Shaaban, S., Hammad, N., Elnemr, A., & Shaaban, I. G. (2023). Efficiency of Bacteria-
1158 Based Self-Healing Mechanism in Concrete. In *Materials Science Forum* (Vol. 1089, pp.
1159 135–143). Trans Tech Publications, Ltd. <https://doi.org/10.4028/p-tc6w54>.
- 1160 [70] Jain, N., Singh, V. K., & Chauhan, S. (2017). A review on mechanical and water
1161 absorption properties of polyvinyl alcohol-based composites/films. In *Journal of the*
1162 *Mechanical Behaviour of Materials* (Vol. 26, Issues 5–6, pp. 213–222). Walter de Gruyter
1163 GmbH. <https://doi.org/10.1515/jmbm-2017-0027>
- 1164 [71] Shen, Y., Li, Q., Xu, S., & Liu, X. (2021). Electromagnetic wave absorption of
1165 multifunctional cementitious composites incorporating polyvinyl alcohol (PVA) fibers
1166 and fly ash: Effects of microstructure and hydration. In *Cement and Concrete Research*
1167 (Vol. 143, p. 106389). Elsevier BV. <https://doi.org/10.1016/j.cemconres.2021.106389>
- 1168 [72] Li, Z., Wang, X., Yan, W., Ding, L., Liu, J., Wu, Z., & Huang, H. (2023). Physical and
1169 mechanical properties of gypsum-based composites reinforced with basalt, glass, and
1170 PVA fibers. In *Journal of Building Engineering* (Vol. 64, p. 105640). Elsevier BV.
1171 <https://doi.org/10.1016/j.jobe.2022.105640>
- 1172 [73] Alderete, N. M., Villagrán Zaccardi, Y. A., & De Belie, N. (2019). Physical evidence of
1173 swelling as the cause of anomalous capillary water uptake by cementitious materials. In
1174 *Cement and Concrete Research* (Vol. 120, pp. 256–266). Elsevier BV.
1175 <https://doi.org/10.1016/j.cemconres.2019.04.001>
- 1176 [74] Martys, N. S., & Ferraris, C. F. (1997). Capillary transport in mortars and concrete.
1177 *Cement and concrete research*, 27(5), 747-760.
- 1178 [75] Aly, T., Sanjayan, J. G., & Collins, F. (2008). Effect of polypropylene fibers on shrinkage
1179 and cracking of concretes. In *Materials and Structures* (Vol. 41, Issue 10, pp. 1741–1753).
1180 Springer Science and Business Media LLC. <https://doi.org/10.1617/s11527-008-9361-2>
- 1181 [76] Akhavan, A., Shafaatian, S.-M.-H., & Rajabipour, F. (2012). Quantifying the effects of
1182 crack width, tortuosity, and roughness on water permeability of cracked mortars. In
1183 *Cement and Concrete Research* (Vol. 42, Issue 2, pp. 313–320). Elsevier BV.
1184 <https://doi.org/10.1016/j.cemconres.2011.10.002>

- 1185 [77] Bear, J. (2013). Dynamics of fluids in porous media. Courier Corporation.
- 1186 [78] Bamigboye, G. O., Ademola, D., Kareem, M., Orogade, B., Odetoyan, A., & Adeniyi,
1187 A. (2022). Durability assessment of recycled aggregate in concrete production. In *The*
1188 *Structural Integrity of Recycled Aggregate Concrete Produced with Fillers and Pozzolans*
1189 (pp. 445–467). Elsevier. <https://doi.org/10.1016/b978-0-12-824105-9.00010-x>
- 1190 [79] R. Siddique and R. Belarbi, (2022). Sustainable Concrete Made with Ashes and Dust from
1191 Different Sources. (2022). Elsevier. <https://doi.org/10.1016/c2020-0-01219-3>.
- 1192 [80] ASTM C1585, (2013). Test Method for Measurement of Rate of Absorption of Water by
1193 Hydraulic- Cement Concretes. ASTM International. <https://doi.org/10.1520/c1585-13>
- 1194 [81] Ataie, F. F., Juenger, M. C. G., Taylor-Lange, S. C., & Riding, K. A. (2015). Comparison
1195 of the retarding mechanisms of zinc oxide and sucrose on cement hydration and
1196 interactions with supplementary cementitious materials. In *Cement and Concrete*
1197 *Research* (Vol. 72, pp. 128–136). Elsevier BV.
1198 <https://doi.org/10.1016/j.cemconres.2015.02.023>
- 1199 [82] Xu, Y., Zhang, X., Ma, B., & Liao, X. (2011). Effects of Temperature on the Performance
1200 of Sucrose in Cement Hydration. In *Journal of Materials in Civil Engineering* (Vol. 23,
1201 Issue 7, pp. 1124–1127). American Society of Civil Engineers (ASCE).
1202 [https://doi.org/10.1061/\(asce\)mt.1943-5533.0000264](https://doi.org/10.1061/(asce)mt.1943-5533.0000264).